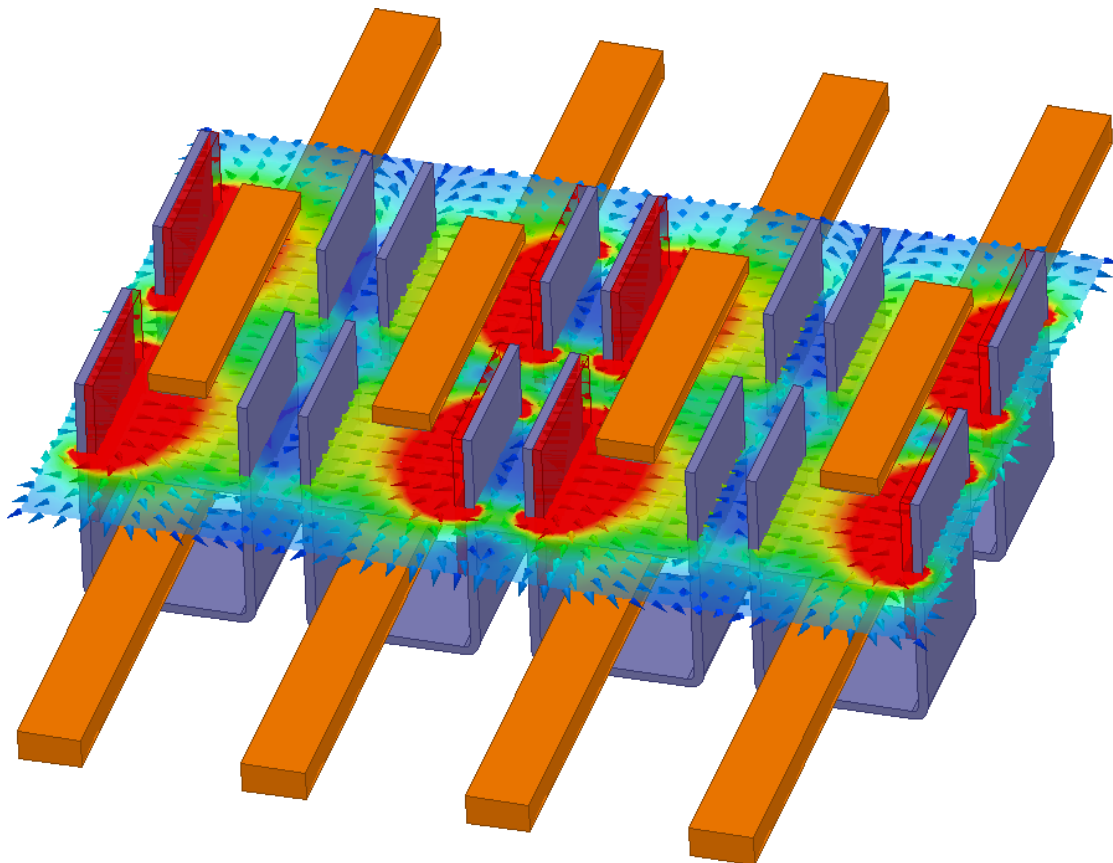


CHALMERS



Pre-Study of Arc Extinguishing Techniques for a 4-Pole 1500 VDC Contactor

Master's Thesis in Applied Physics

ALFRED NILSSON

Department of Applied Physics
CHALMERS UNIVERSITY OF TECHNOLOGY
Gothenburg, Sweden 2014

Abstract

A contactor is an electronically controlled switch used for switching a power circuit. The principles have been the same for a hundred years, i.e. there is a contact system that does the job. The contactor is operated by a control voltage that causes it to open or close. Common applications include starting and stopping of short-circuited motors, purely resistive loads, and bypass applications. These are all usually AC applications.

The recent emergence of solar energy applications has increased the demand for products that can also handle DC. The difficulty with DC is to break the current. Unlike a direct current, an alternating current will have a zero-crossing point at every half cycle. During this period of low current, the arc can be extinguished with relative ease by preventing re-ignition of the arc. For DC however, the current remains constant over time and the breaker needs to attenuate the flow of current. When the contacts are separated an electric arc occurs between them which has to be extinguished in some way for the current to be broken. This makes DC breaking extra difficult and special features need to be implemented in order to extinguish the arc and break the current flow. High voltage electric arcs causes significant damage to the electrodes and shorten the lifetime of the contactor. Therefore, minimizing the arc duration time is an important engineering challenge.

This thesis is a pre-study of arc extinguishing techniques for a DC contactor. The goal is to be able to break 1500 VDC using 4-poles connected in series. This thesis project is divided into two parts.

In the first part of the project, permanent magnets were used to suppress the arc and the simulations were performed in *ANSYS Maxwell*. The method considered all possible wirings of the contactor and compared the results to an existing 3-pole DC contactor. The proposed optimal solution uses steel plates surrounding the magnet and contact system to increase the magnetic flux density. Results show an increased efficiency of the magnets used by 164.8%.

In the second part of the projects, a DC arc model was implemented in the computer program *ANSYS Simplorer* using theory found in literature. The model was extended to a model of 4-pole 1500 VDC contactor. The model successfully simulates the current-voltage characteristics of the contactor during the breaking process and predicts critical currents.

Keywords: Contactor, DC Switching, ANSYS Maxwell, ANSYS Simplorer, Electric Arc, Arc Extinguishing, Arc Modelling

Acknowledgements

I would like to thank Tobias Gentzell, Krister Linnarud and Lena Borg for all the administration work that made this thesis work possible. Thanks to everyone working at ABB Control Products in Västerås for all your helpfulness and friendly atmosphere.

Special thanks to my supervisor David Karlén at ABB and my examiner Magnus Karlsteen at Chalmers for all of your guidance and help. Thanks to Mats Johansson for helping me search for old documents and Staffan Palm for your insights as an electronics designer.

I would also like to thank the other thesis workers Markus Angell, Oscar Ericsson, Dan Tjerngren and Jon Tjerngren for the company and camaraderie over the last five months.

Lastly I will acknowledge the support from my family and loved ones which kept me motivated through my studies and through this project.

Alfred Nilsson, Västerås 2014-05-30

Contents

1	Introduction	1
1.1	About ABB	1
1.2	Increasing Demand for DC Power	2
1.3	The Contactor	2
1.3.1	Operating Principle	3
1.3.2	Different Models	5
1.3.3	AF-contactor Sizes	5
1.4	Project Background	6
1.5	Purpose and Limitations	6
1.5.1	Part I: Permanent Magnets	6
1.5.2	Part II: DC Arc Model	7
2	Theory	8
2.1	The Electric Arc	8
2.1.1	Plasma	8
2.1.2	Formation of the Arc	8
2.1.3	Arcing in Air at Atmospheric Pressure	10
2.1.4	Minimum Arc Current and Voltage	11
2.1.5	Current-Voltage Characteristics of the Arc	12
2.2	Consequences of Arcing	12
2.2.1	Contact Erosion	12
2.3	Magnetism in Contactors	13
2.3.1	Arc Mobility	14
2.4	Arc Interruption	16
2.4.1	Arc Suppression Using Permanent Magnets	17
3	ANSYS Maxwell Simulations	18
3.1	Computation	18
3.2	GAF185-30	18
3.2.1	Design	19

3.2.2	Simulation model	20
3.3	Wiring Diagrams	21
3.4	Magnetic Guides	22
3.5	Simulation Models	24
3.5.1	Without Steel Plates	25
3.5.2	With Steel Plates	27
4	ANSYS Simplorer Simulations	29
4.1	About Simplorer	29
4.2	DC Arc Model	29
4.2.1	Free-burning Arc	30
4.2.2	Arc inside Chamber	30
4.2.3	Arc Motion	30
4.3	Simplorer Model	32
4.4	4-Pole Model	34
5	Maxwell Simulation Results	36
5.1	GAF185	36
5.2	w/o Steel Plates	37
5.2.1	RLRL	37
5.2.2	RLLR	38
5.2.3	RRLR	38
5.3	With Steel Plates	39
5.3.1	RLRL	39
5.3.2	RLLR	40
5.3.3	RRLR	40
5.4	Summary	41
6	Simplorer Simulation Results	42
6.1	1-Pole Model	42
6.2	4-Pole Model	44
7	Discussion	46
7.1	Part I	46
7.1.1	Conclusions	47
7.1.2	Recommendations for future work	47
7.2	Part II	48
7.2.1	Conclusions	48
7.2.2	Recommendations for future work	48
	Bibliography	50

1

Introduction

A CONTACTOR is an electronically controlled switch used for switching a power circuit. The principles have been the same for a hundred years, i.e. there is a contact system that does the job. The contactor is operated by a control voltage that causes it to open or close. Common applications include starting and stopping of short-circuited motors, purely resistive loads, and bypass applications. These are all usually AC applications.

The recent emergence of solar energy applications has increased the demand for products that can also handle DC. The difficulty with DC is to break the current. When the contacts are separated an electric arc occurs between them which has to be extinguished in some way for the current to be broken. High voltage electric arcs causes significant damage to the electrodes and shorten the lifetime of the contactor. Therefore, minimizing the arc duration time is an important engineering challenge. That is the starting point of this thesis project.

1.1 About ABB

ABB (*Asea Brown Boveri*) is a world leader in power and automation technologies, operating in over 100 countries with approximately 150,000 employees.

This thesis work was conducted at ABB Control Products in Västerås, Sweden. Control Products is part of the Low Voltage Division which manufactures systems and products that provide control, measurement and protection for electrical installations, electronics, switchboards, enclosures and electromechanical devices for industrial machines and plants. Low voltage is defined as voltages up to 1000 V AC or 1500 V DC.

Control Products in Västerås have around 350 employees and revenues about 1.5 billion SEK annually. The main products are contactors, soft-starters and pilot devices.

1.2 Increasing Demand for DC Power

In the year 2000, DC type loads covered merely 10% of all the electricity loads. However, due to the rapid expansion of computers and digital devices, DC type loads is estimated to cover 50% in 2020 [1]. The expansion of renewable energy systems and applications also contributes to this acceleration. The advantage of DC distribution systems is that DC type loads are more easily interfaced with a DC grid, compared to an AC grid where the current first has to be converted.

Although these are high voltage loads, the recent emergence of solar energy applications has also increased the demand for products that can also handle low voltage DC. A reliable DC system require dedicated DC contactors to control and break the current. However, interrupting a direct current is difficult as it is continuously flowing and has no point where it crosses zero as in the case of AC.

1.3 The Contactor

Contactors are typically designed to be connected directly to high current loads. Unlike relays, they are made to withstand higher current ratings and being able to switch circuits rated for several kilowatts. To do this a contactor is designed with features to control and suppress the electric arc formed during the breaking process.

One *pole* refers to a whole contact system including *arc chamber* as illustrated in Figure 1.1. The arc chambers consists of several stacked metal plates called *lamellae*. The function of these lamellae is explain in Section 2.4. The contact system consists of two stationary conductors and a mobile conductor, all made out of copper and with $AgSnO_2$ contact pads. On top of the mobile conductor is the *arc beam* which is attached to a *contact bridge* allowing it to move. The purpose of the arc beam is to allow the electric arc to move away from the contacts and reach more lamellae. An arc situated between the two contacts is called a *free-burning arc*, see left contact in Figure 1.1. An arc which has split into several smaller arcs between the lamellae is said to be *inside the arc chamber*, see right contact in Figure 1.1

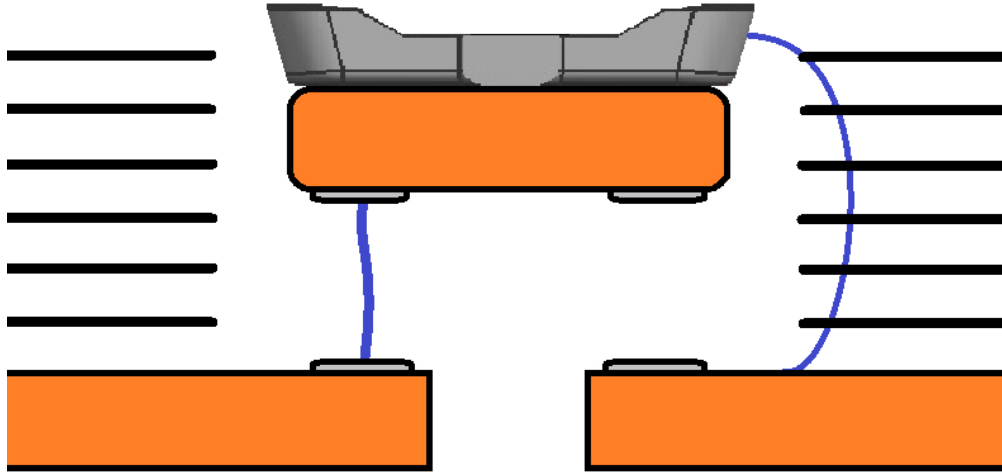
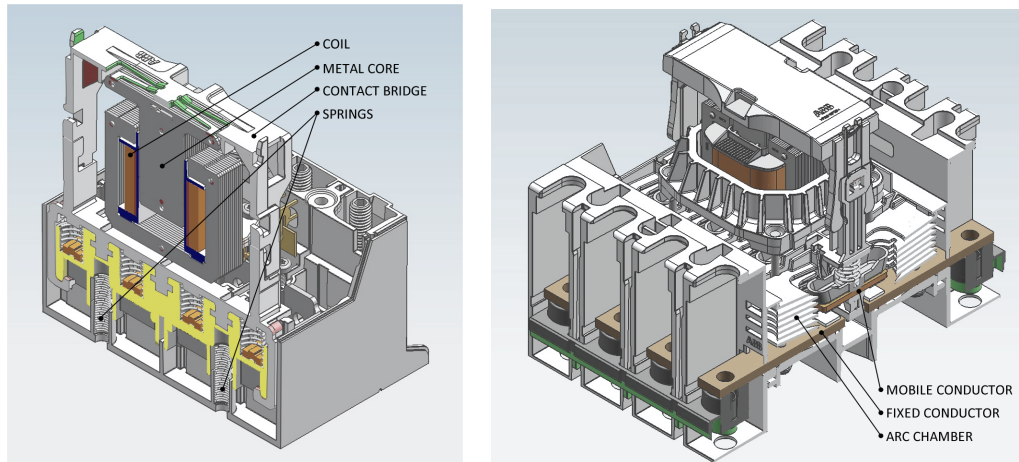


Figure 1.1: One pole includes contact system and arc chamber. An arc could be free-burning (left) or it could be inside the arc chamber (right).

1.3.1 Operating Principle

The contact system is quite simple and the principles has remained the same for a hundred years. The contactor is constructed as "normally open" so that the contacts are separated by a spring mechanism. When a control current passes through the electromagnet, it induces a magnetic field which attracts the moving metal core inside the contactor. The metal core is connected to the mobile conductors through a contact bridge as shown in Figure 1.2(a). The force overcomes the spring forces and the moving conductors are forced into contact with the fixed contacts.

Figure 1.2(b) shows another view of how the contact bridge is connected to the metal core inside the coil. Also visible on the side of the contacts are the *arc chambers*, consisting of several stacked metal plates called *lamellae*.



(a) A mid cross section reveals how the metal core connects to the contact bridge. (b) One of the outer poles visible with arc chamber, mobile and stationary conductors marked.

Figure 1.2: Actual drawing of an AF-contactor with the plastic covers removed to display the inner parts.

The complete assembly consists of many working parts as seen in Figure 1.3. It could be helpful to understand how the contactor is constructed, but only the contact systems and arc chambers are concerned in this thesis project.

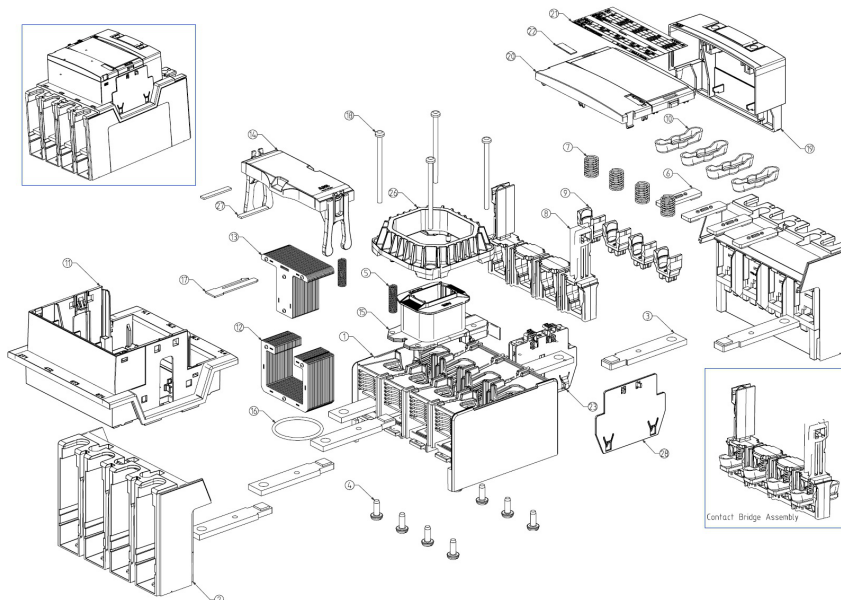


Figure 1.3: Exploded view of a complete contactor.

1.4 Project Background

Unlike a direct current, an alternating current will have a zero-crossing point at every half cycle. During this period of low current, the arc can be extinguished with relative ease by preventing re-ignition of the arc. For DC however, the current remains constant over time and the breaker needs to attenuate the flow of current. This makes DC breaking extra difficult and special features need to be implemented in order to extinguish the arc and break the current flow.

Solar energy generates DC power which needs to be converted to AC to match the power grid. For safe operation, the current needs to be controlled on both sides of the power inverter. Many applications today are at 1000 V but the development is shifting towards 1500 V, increasing the demand for ABB's products to meet these requirements. ABB is planning to develop a 4-pole DC contactor which, with all poles connected in series, could handle DC breaking up to the required 1500 V.

1.5 Purpose and Limitations

The main objective of this thesis is to conduct a pre-study on suitable technologies for DC switching. The project is divided into two parts. The first part is to design and evaluate a technical solution using permanent magnets. The second part is to develop a simulation model of a 4-pole DC contactor.

General Limitations

This thesis work is purely a simulation project and the generated results will consist of simulation data. No new measurements will be performed during this project and no prototypes will be built.

1.5.1 Part I: Permanent Magnets

Permanent magnets are placed in the vicinity of the contact system. The electric arc that occurs will be affected by a force that leads it away from the contacts and into an arc chamber that extinguishes it (see Section 2.3 and 2.4.1). The additional magnetic flux will assist the critical currents, which themselves do not generate a strong enough field. This is a well-known technique that ABB already uses for an existing 3-pole contactor. The performance of this contactor will be used as a benchmark for evaluating the results.

The task here is to simulate and compare different configurations of magnets. The goal is to find an efficient solution, both in performance and cost. Simulations will be performed in *ANSYS Maxwell*.

Limitations

The simulations are performed at already maximum opening distance. The arc is assumed to be a solid cylindrical conductor and stationary located between the center of

the contacts. Simulations will only analyze the efficiency of the design, not how it affects the electric arc. The arc is assumed to be effectively extinguished if it reaches the arc chamber.

1.5.2 Part II: DC Arc Model

The task is to implement a model to simulate the current-voltage behaviour of a DC contactor. Literature studies will be conducted to find relevant theory and equations used for the model. Simulations will be performed in *ANSYS Simplorer*.

Limitations

The extent of all simulation models are limited by models and theory found in literature. No new measurements or experimental research will be performed. Factors less relevant for the current-voltage behaviour will be excluded from the model to reduce the complexity and improve simulation times.

2

Theory

2.1 The Electric Arc

An electric arc will always occur between two opening contacts if the circuit current and the voltage across the contacts are above certain minimum values (see Section 2.1.4). The arc appears as a bright shining shape between the contacts. It acts as an electrical conductor and as long as the arc is present the circuit will be closed.

2.1.1 Plasma

Plasma is the fourth fundamental state of matter with the other being solid, liquid and gas. Although it seems uncommon in our everyday life, plasma is the predominant state of all the matter in the universe as most stars and intergalactic gas are in a plasma state.

When sufficient heat is added to a gas the electrons will break free from the atoms. This creates a system of negative charged electrons and positive charged ions with equal charge densities. Although unbound, the particles are not free in the sense that their motion generates magnetic fields affecting each other. The plasma occurring when the ionized gas between two electrical contacts is ignited is called an electric arc. This thesis will not immerse deep into the theory of plasma physics, but it is important to understand the basic to understand the formation and behaviour of the *electric arc*.

2.1.2 Formation of the Arc

The arc always initially forms from the metal vapours from the contacts themselves and the formation depends entirely on the properties of the contact material. It is natural to assume that two contacts are in smooth contact over the whole contact area, however this is not the case. A microscopic view would reveal irregularities in the material and the electrical contact will only be established in a few places known as *contact spots* or *a-spots*. See Figure 2.1.

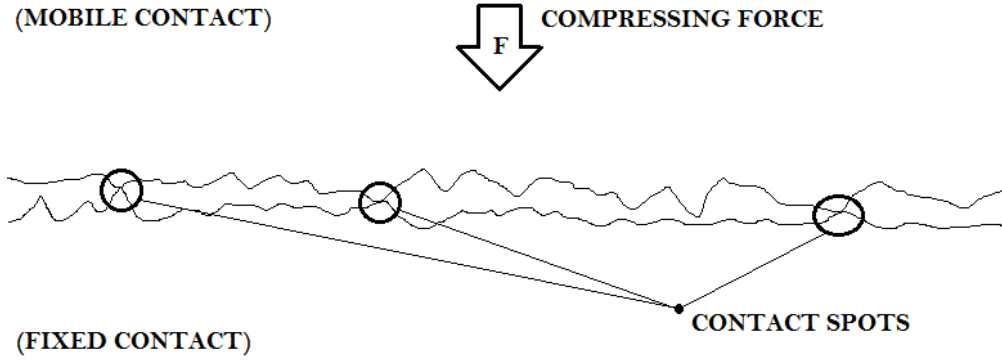


Figure 2.1: Microscopic view of the boundary between two contacts.

The contact spot area, A_{cs} , will decrease as the contacts separate as:

$$A_{cs} \propto \frac{F}{H} \quad (2.1)$$

Where F is the compressing force and H is the hardness of the material. The temperature of the contact spot will increase rapidly as all current is concentrated into a smaller area. When the contact spot temperature reaches the melting temperature of the metal, T_m , a molten bridge will be formed between the two contacts. The molten bridge will be stable and continue to lengthen with the separating contacts until the temperature reaches the boiling temperature of the metal, T_{bl} . At this point the bridge ruptures and the hot metal gas is released into the space between the contacts. The conditions are such that thermal ionization can take place and the temperature at the cathode region is sufficient for effective liberation of electrons. Therefore, after the bridge ruptures and the voltage across the contacts are greater than some minimum value, U_{min} , (see Section 2.1.4) an electric arc will form immediately [3]. The whole opening sequence is illustrated in Figure 2.2.

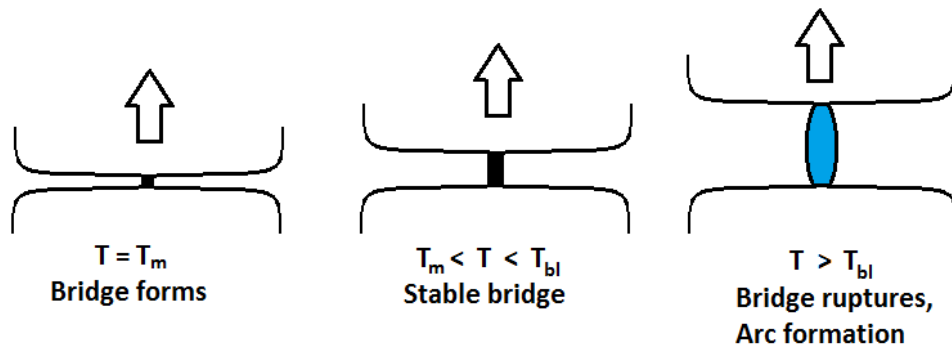


Figure 2.2: The three stages of arc formation during the separation of contacts.

An electric arc formed on opening the contacts is called a *break arc* and an arc formed

on closing the contacts is called a *make arc*. Generally, a break arc is more harmful to the device as it typically has a longer arcing time.

2.1.3 Arcing in Air at Atmospheric Pressure

This thesis will only consider arcing in air at atmospheric pressure, as this is the case for all of ABB's contactors. Some contactors operate in a gas or oil environment, however the same theory is valid for them.

Figure 2.3 shows a generic electric arc. It has a voltage drop at the cathode, U_c , and another voltage drop at the anode, U_a . U_c is typically greater than U_a and these regions are referred to as the *Cathode Fall* and the *Anode Fall* respectively. Between them the *Arc Column* [3].

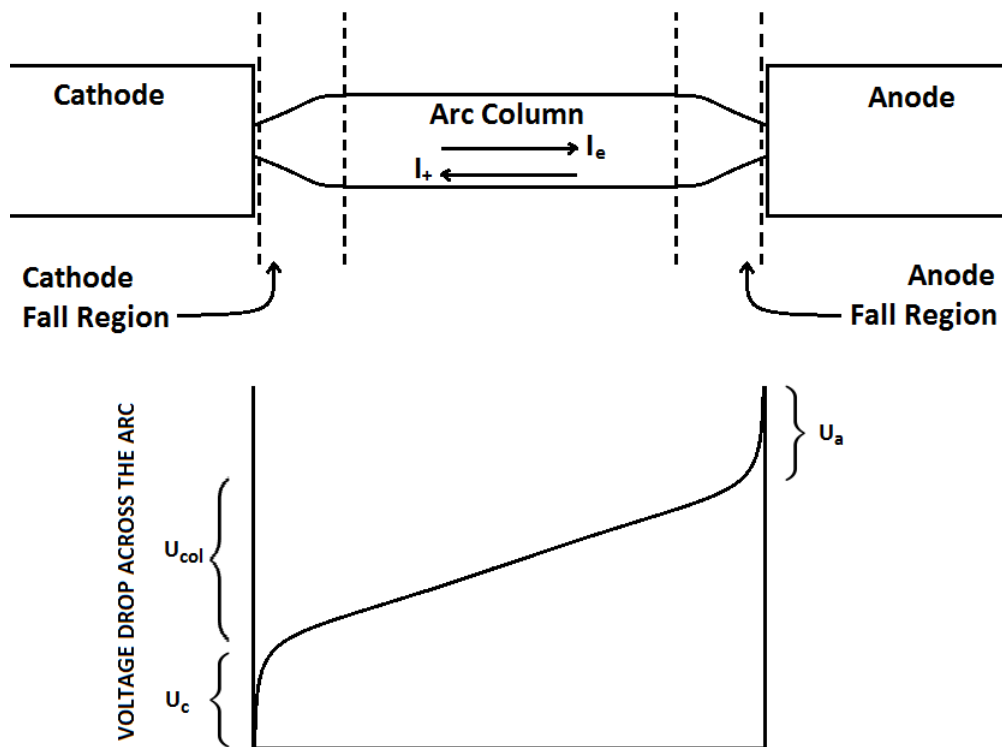


Figure 2.3: Schematic depicting a generic arc. The three main regions along with the flow of current and electrons are illustrated. Voltage drop across the arc is shown below [3, p.456].

The Cathode Region

The cathode fuels the arc with electrons which allows it to continue burning between the contacts. If the supply of electrons to the cathode does not exceed a minimum value (see table 2.1) the energy losses will be greater than the introduced energy and the arc

will be extinguished.

The voltage drop across the cathode is typically between 8 V and 15 V [3]. This depends on material and the surrounding gas.

The Anode Region

The anode collects the electrons emitted by the cathode. The temperature, current density and voltage drop across the anode fall is generally lower than for the cathode [3].

The Arc Column

In the arc column the density of ions and the density of free electrons are equal, thus it has plasma characteristics. Unlike the fall regions the arc column voltage drop is not constant, but length dependent. A longer arc consists of more plasma and increases the voltage. The voltage increase, $E(I_A, d)$ [V cm^{-1}], is a function of both the contact gap and the arc current. It is important to not that the arc voltage is determined by the input power required to sustain the electric arc, and not the circuit or system voltage.

2.1.4 Minimum Arc Current and Voltage

An already established arc requires a continuous flow of electrons from the cathode to be sustained. Below some minimum value $I_A \leq I_{min}$, the energy losses will exceed the introduced energy to the cathode and the arc will be extinguished.

A minimum voltage, U_{min} , is also required across the open contacts to sustain the arc. The electric arc would at least require a voltage that corresponds to the ionization potential of the gas, V_i , and the work function voltage, U_ϕ , of the cathode contact. It is therefore reasonable to assume that [3]

$$U_{min} \approx V_i + U_\phi$$

Calculated values for $V_i + U_\phi$ is compared to measured value for U_{min} and also I_{min} for different contact materials in Table 2.1.

	V_i (volts)	U_ϕ (volts)	$V_i + U_\phi$ (volts)	U_{min} (volts)	I_{min} (amperes)
Al	5.98	4.10	10.08	11.2	0.4
Ag	7.57	4.74	12.31	12	0.4
Cu	7.72	4.47	12.19	13	0.4
Fe	7.90	4.63	12.53	12.5	0.45

Table 2.1: The minimum arc current (I_{min}) and minimum arc voltage (U_{min}) compared to the sum of the ionization potential and the work function potential ($V_i + U_\phi$) and for various contact materials. Taken from [3, p.464]

2.1.5 Current-Voltage Characteristics of the Arc

The total arc voltage U_A is given by the sum of the cathode fall voltage, the column voltage and the anode fall voltage, shown in Figure 2.3:

$$U_A = U_c + U_{col} + U_a \quad (2.2)$$

The column voltage depends on the length of the arc and the arc current. [3] gives a model for the voltage, U_A , across a free-burning arc obtained from measurement data

$$U_A = \Delta + (\tau + d) \cdot b \ln^{-3} \frac{I}{q} \quad (2.3)$$

where I is the arc current and d is the arc length. From the literature it can be found that for silver contacts $\tau = 1.1$ cm, $b = 5400$ Vcm⁻¹ and $q = 7.4$ mA. Δ is the anode and cathode fall voltages retrieved from table 2.1.

2.2 Consequences of Arcing

The presence of an electric arc has both positive and negative consequences. The positive aspect is that the arc allows for a smooth decrease to zero current. If the circuit current were to suddenly drop to zero at the moment of contact separation, the energy stored in the inductance, L , would cause an over-voltage given by

$$V = -L \frac{dI}{dt} \quad (2.4)$$

The presence of an electric arc usually limits the over-voltage to a maximum of two or three times the circuit voltage. Without this feature, switch designers would have to design to protect the circuit against large over-voltages.

However, other consequences of arcing could be devastating for the switching device and affects the design and choice of materials.

2.2.1 Contact Erosion

Erosion of the contact material is one of the most important consequences of arcing to design for as it directly relates to the lifetime of the device. It occurs because both the anode and cathode heats up to above the boiling temperature of the contact material. The temperature of the arc is so high that erosion occurs even if the arc is moving across the contact surfaces. The amount of erosion depends on many parameter, for example:

- Circuit current
- Arcing time
- Open gap distance
- Contact material

- Size and shape of the contact
- Contact opening velocity
- Arc motion on the contacts
- Design of the arc chamber

2.3 Magnetism in Contactors

The Biot-Savart law describes the magnetic field generated by an electric current, typically through a wire.

$$\vec{B} = \frac{\mu_0}{4\pi} \oint_C \frac{IdL \times \vec{r}}{|\vec{r}|^3} \quad (2.5)$$

Where \vec{B} is the generated magnetic flux density, I is the current, L is the length of the arc and \vec{r} is the displacement vector from the point at which the field is being computed to the wire. The self-induced magnetic field inside the contactor is referred to as the *magnetic blast field*.

The arc current flowing perpendicular to this magnetic field will experience a Lorentz force causing it to move, usually into an arc chamber. The Lorentz force acting on the arc can be obtained by equation 2.6.

$$\vec{F} = \int_{V_a} \vec{J}_a \times \vec{B} dV_a \quad (2.6)$$

Where \vec{J}_a is the current density and V_a the arc volume.

Figure 2.4 illustrates the desired direction of the magnetic field in order to have a net Lorentz force towards the arc chambers. In a simple contact system, as displayed in the figure, the arc will experience a magnetic field induced from the stationary contact, the mobile contact and from the arc on the opposite side (negligible due to the large distance). However, the magnetic field contributions from the stationary and mobile contact cancels out as they are approximately equal in magnitude and have opposite direction (easily verified with the right-hand rule). In order to have a net magnetic blast field according to Figure 2.4 the contact systems have to be carefully designed to influence the magnetic field around the contact area. This feature is usually integrated with the arc chamber. In AC, eddy currents are induced in the lamellae creating the magnetic blast field. Typical values for the magnetic blast fields are a few tens of mT for every thousand amperes in arc current.

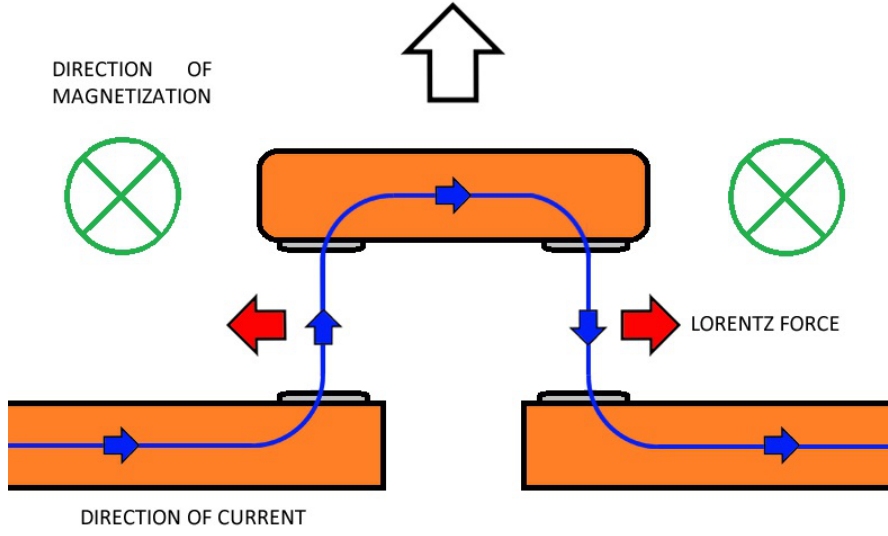


Figure 2.4: Direction of currents through fixed and mobile conductors and contacts. The magnetization arrows indicates the desired direction of the magnetic field in order to have outward directions of the Lorentz force.

2.3.1 Arc Mobility

The driving force of the arc, expressed in equation 2.6, can be written simply as

$$F = B_y I L \quad (2.7)$$

Given that the arc is assumed to be a straight conductor of length L , and B_y being the magnetic flux component that intersects the arc according to Figure 2.4, and I being the arc current. The equation of motion for the arc is given by

$$F - F_f = m \frac{dv}{dt} \quad (2.8)$$

where F_f is the frictional force on the arc, v is the arc velocity and m is the mass of the arc. If the friction between the arc and the contacts is neglected and only the drag force in the air is considered, F_f is given by [4]

$$F_f = C_D \frac{\rho v^2 D L}{2} \quad (2.9)$$

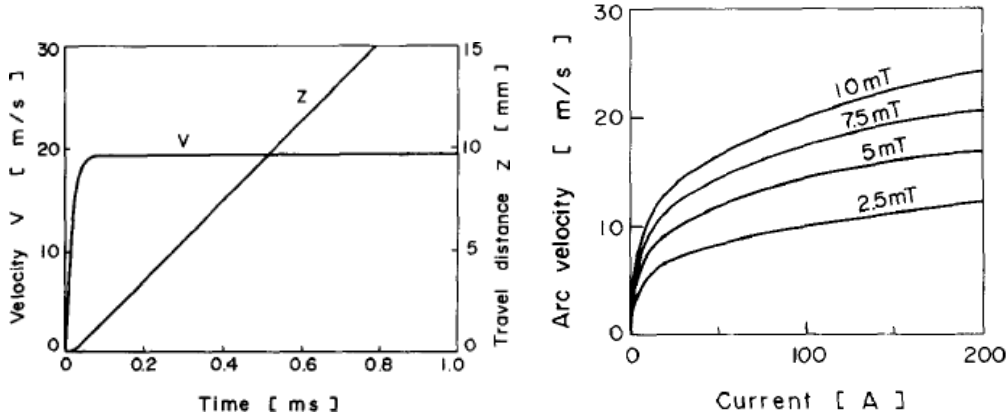
where D is the arc diameter, L is the arc length, ρ is the density of air, and C_D is the drag coefficient. Assuming a cylindrical shape of the arc, the drag coefficient is approximately [4]

$$C_D = 0.62 \left(\frac{L}{D} \right)^{0.12} \quad (2.10)$$

Assuming that the arc consists of electrons and singly ionized atoms the mass can be estimated as

$$m = \left(\frac{M}{N_A} \right) \times \left(\frac{\pi}{4} D^2 L \right) \times \left(\frac{P}{2k_B T} \right) \quad (2.11)$$

Mori et al [4] calculated the velocity and travel distance of the arc using the parameters $I = 100$ A, $B = 10$ mT, $L = 5$ mm, $J \approx 2.5 \times 10^6$ A/m², $P = 1$ atm, $T = 20,000$ K and $\rho = 1.3$ kg/m³ (for air), $M = 108$ g/mol (for silver) and the result is shown in Figure 2.5(a).



(a) Velocity and travel distance of the arc with $B = 10$ mT and $L = 5$ mm. (b) Arc velocity as a function of current for several B-fields and $L = 4.5$ mm.

Figure 2.5: Arc velocities calculated by [4] using the equations derived above.

As seen in Figure 2.5 the velocity increases rapidly in time to reach a saturation velocity. In the case described above, saturation velocity was reached in less than 0.1 ms and calculated to be around 20 m/s.

Knowing that $dv/dt = 0$ after saturation, and assuming $J = I_A/(\pi D^2/4)$, equations (2.7)-(2.10) can be rearranged to find the saturation velocity, V_s :

$$V_s = 1.80 \frac{J^{0.22} B^{0.5} I_A^{0.28}}{\rho^{0.5} L^{0.06}} \quad (2.12)$$

Figure 2.5(b) shows V_s as a function of current for different magnetic flux densities.

Mori also compared his calculations with previous measurements and found they agree quite well. However, in the derivation of (2.12) the arc was assumed to be a rigid straight conductor which of course is not the case. The anode and the cathode regions of the arc can have different velocities and in most cases the cathode region experience more resistance to start moving.

Limits for continuous motion

Measurements have been performed in order to determine the limits for reliable magnetic blowout at different currents [5]. Smooth drifting of the cathode region is allowed if:

$$B[\text{mT}] \cdot d[\text{cm}] \cdot I_A^{0.63}[\text{A}] > 20 \quad (2.13)$$

[5] also concludes that the cathode region will not be able to move if:

$$B[\text{mT}] \cdot d[\text{cm}] \cdot I_A^{0.63}[\text{A}] < 9 \quad (2.14)$$

The drift velocity of a free-burning arc will depend on the opening gap if [6]

$$B \cdot L^3 < 0.3 \quad (2.15)$$

The expected value of the drift velocity is then given by

$$v = 0.305 \cdot I_A^{0.6} B^{1.4} L^{2.22} \quad (2.16)$$

This is only an approximation and the drift velocity can vary a lot. However, if $B \cdot L^3 > 0.3$ the drift velocity is independent of the opening gap and is given by

$$v = 0.176 \cdot I_A^{0.61} B^{0.74} \quad (2.17)$$

2.4 Arc Interruption

A DC circuit at the moment of interruption with a burning electric arc across the contacts is assumed to be represented in the model according to Figure 2.6. U_A is the voltage drop over the electric arc.

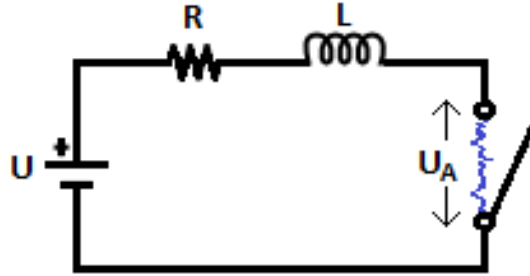


Figure 2.6: DC circuit model with an electric arc between the open contacts.

$$U = Ri + L \frac{di}{dt} + U_A \quad (2.18)$$

Initially, $U = Ri$ and U_A must be equal to zero. At $t = 0$ when the arc is initiated, $dI/dt = -U_A/L < 0$. At some point $U - Ri = U_A$, dI/dt will equal to zero and the current will cease to decrease. At this point a stable burning arc will exist.

Breaking the current requires that $U_A > U - Ri$. In order to have quick current interruption a high arc voltage, U_A , has to be achieved in a short amount of time. High arc voltages can be achieved in three different ways:

Cooling

The voltage is increased by removing energy from the arc.

Extension

Extending the length of the arc column increases the total voltage as described by Equation (2.3). However, a pure extension of the arc could only be used to break small currents. Larger current would require substantial length in order to be extinguished.

Split the arc into sub-arcs

An effective way to increase the arc voltage is to split the arc into several arcs. Equation 2.18 can be modified for n number of arcs:

$$U = Ri + L \frac{di}{dt} + n \cdot U_A$$

This differential equation yields the number of arc splittings required to achieve a break-time t_c :

$$n = \frac{U}{U_A} \frac{1}{1 - e^{-t_c/T}}$$

where T is the time constant of the circuit L/R . Splitting of the arc happens between the lamellae in the arc chamber. To split the arc into n sub-arcs, $n - 1$ lamellae are needed. The distance between the lamellae is quite small (< 3 mm) in which case each sub-arc will have a voltage drop of about 25 V [6]. It is therefore easy to calculate the minimum number of sub-arcs needed to break 1500 V over four poles (eight contacts):

$$n_{min} = \frac{1500/8}{25} = 7.5 \leq 8 \quad (2.19)$$

To achieve eight sub-arcs, a minimum of seven lamellae are needed at each contact.

2.4.1 Arc Suppression Using Permanent Magnets

The presence and purpose of magnetic blast fields inside a contactor was described in Section 2.3. However, lower currents will in turn generate smaller blast fields which could compromise the mobility of the arc (as described in Section 2.3.1). Currents unable to move into the arc chamber could remain as free-burning arcs between the contacts for a significant amount of time. There are referred to as *critical currents* and can cause major damage to the device and could even be a fire hazard [7].

Placing magnets in the vicinity of the contact system would ensure that a permanent magnetic field is present to mobilise the electric arc. Several studies have been performed to study the effects as the magnetic field lengthens the arc [8, 9, 10, 11]. However in this thesis the main objective is not the achieve arc extinction solely through lengthening of the arc, but to move it into the arc chamber. The permanent magnets need to be placed in such manner that the magnetic field is sufficiently strong to ensure smooth arc drifting for all critical currents, according to the criteria set in Section 2.3.1.

3

ANSYS Maxwell Simulations

The first part of this thesis project was to study and evaluate a technical solution of using permanent magnets. The purpose with the external magnetic field is for the electric arc to experience a Lorenz force which helps accelerating it into the arc chamber. This is a known technique and is currently used by ABB.

3.1 Computation

The tool used for simulations is ANSYS Electromagnetics, also known as ANSYS Maxwell or Maxwell 3D. It is a powerful computer program design to solve electric, magnetostatic, transient and eddy current problems. This is done using finite element methods to divide the model into a mesh with a finite number of discrete areas and solving Maxwell's equations for each element. The program refines the mesh at every iteration in order to find a solution which is numerically stable. Numerical stability implies that an input error is not magnified during the calculations.

The magnetostatic solver was used in this thesis. The calculations were set to iterate until the energy error was less than 1%, with 30% refinement of the mesh for every iteration.

3.2 GAF185-30

The GAF185 is a 3-pole contactor in ABB's product line which has been reconstructed from an AC to a DC contactor. The DC version uses permanent magnets for arc suppression as described in Section 2.4.1. It has the same physical size as the AF205 (internally referred to as Size 5) making it ideal to use as a benchmark for my simulations. The goal of this part of the project is to propose an arrangement of magnets which is as, or more, efficient than the GAF185.

Since the GAF contactor has three poles, and the contactor concept in interest will have four poles, some key indicators will be of interest.

— Volume of magnets used per pole:

$$V_{Magnets}/N_{Poles} \quad (3.1)$$

This is a fairly important factor as the magnets are costly and a good design should use as few magnets as possible.

— Average effective B-field:

$$\langle B_y \rangle = \frac{1}{V} \int_V B_y dV \quad (3.2)$$

B_y is the magnetic flux in \hat{y} direction as in Figure 2.4. V is the volume around the contacts where the arc is likely to appear. In the simulations, this volume is chosen to be a rectangular box situated between the stationary and mobile contact pads. These contact pads have an area of about $9 \text{ mm} \times 9 \text{ mm}$ and simulations are performed at the maximum opening distance of 12 mm .

3.2.1 Design

The overview design of GAF185 can be seen in Figure 3.1. To the right, the arc chute is displayed separately and the vacancies for the magnets are visible. Neodymium magnets are used with the size $25 \times 25 \times 1.5 \text{ mm}$.

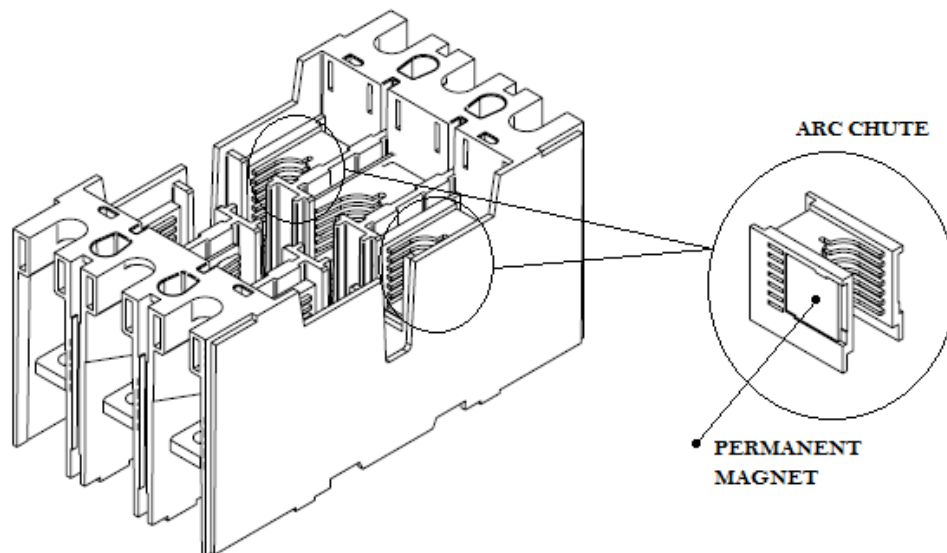


Figure 3.1: (Left) GAF185-30 complete bottom part. (Right) Arc chute for the outer poles with space for the magnets.

Since magnets are only used for the outer two poles, and not for the inner one, a total of eight magnets are used. Figure 3.2(a) shows a top view of the assembly and the direction of the magnetization.

The simplest wiring diagram of a 3-pole contactor is illustrated in Figure 3.2(b). It is easy to see that the direction of the magnetization has to be reversed for the middle pole in order for the Lorentz force to be directed outwards. Since this is not satisfied by the GAF185 design, effective arc extinguishing will only occur at two out of the three poles.

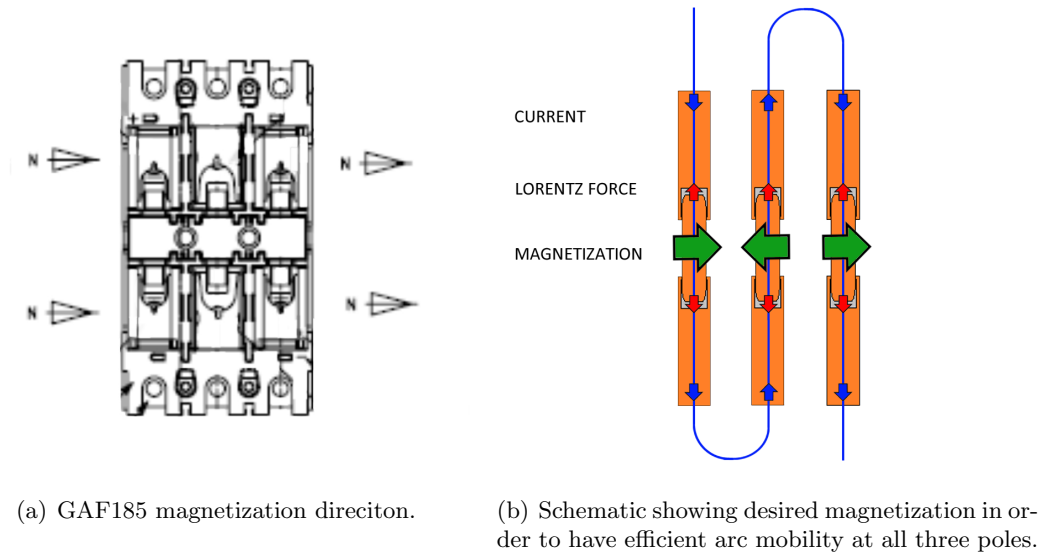


Figure 3.2: *GAF185-30 blueprint and a wiring diagram.*

3.2.2 Simulation model

Using the actual sizes and dimensions from the GAF185 blueprints a model was implemented in ANSYS Maxwell. Most components serve no magnetic purpose and were therefore not included in the model, this significantly improves computing time. The components included were the permanent magnets, the fixed and mobile conductors and contacts. The electric arc is modelled as a straight cylindrical conductor. See Figure 3.3.

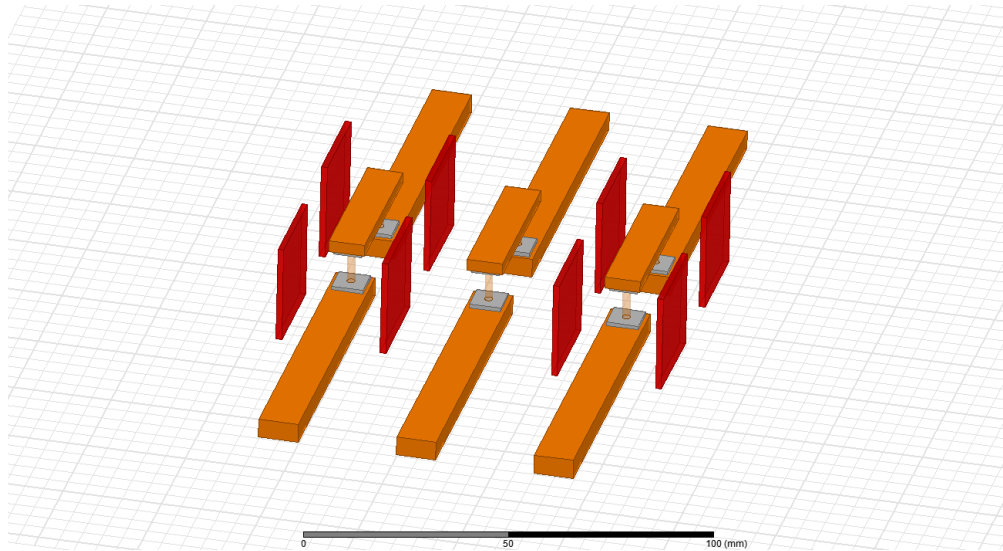


Figure 3.3: *GAF185 simulation model.*

3.3 Wiring Diagrams

The number of ways to wire a 4-pole contactor is $4! = 24$. However most of these are redundant as they will give rise to identical, or identical but mirrored, current paths. One restriction is the reluctance to connect to the opposite side of the device, as this would require external cables to wrap around the device. Contactors are often installed close to each other in cabinets and additional cables would interfere with the installation.

The possible connections will consist of those that have two current paths downwards and two upwards. The total number of configurations are therefore $\binom{4}{2} = 6$. However, due to symmetry the first three configurations will be equivalent to the last three with reversed current direction, which would be equivalent to reversing the direction of the magnets.

Three unique configurations were therefore studied as seen in Figure 3.4. The current paths will be Down-Up-Down-Up, Down-Up-Up-Down, and Down-Down-Up-Up. The desired magnetization directions will be Right-Left-Right-Left (RLRL), Right-Left-Left-Right (RLLR), and Right-Right-Left-Left (RRLL) respectively.

The three simplest wirings to achieve these configurations are shown in Figure 3.5.

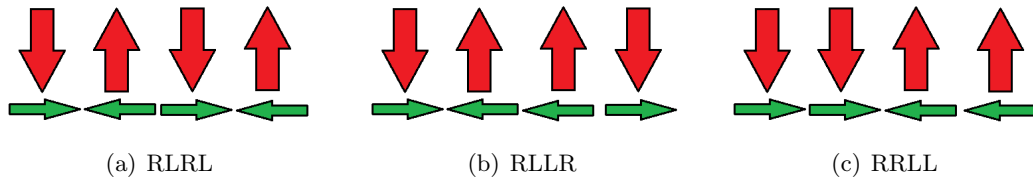


Figure 3.4: Red arrows depicting upwards or downwards flow of current. Green arrows depicting the direction of magnetization in order to have a Lorentz force towards the arc chamber.

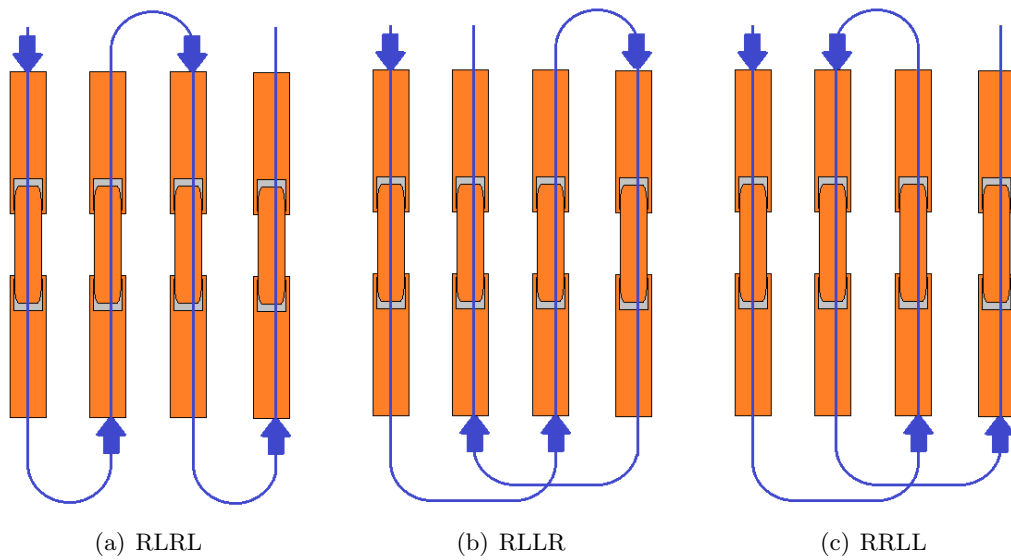


Figure 3.5: Three simple wiring schematics to have the currents flow as shown in Figure 3.4.

3.4 Magnetic Guides

A major issue from using permanent magnets, as discussed before, is that magnetic flux from neighbouring poles interfere with each other. One idea is to use curved metal plates around the magnets to create an enclosed magnetic circuit. This should in theory increase the magnetic flux density within the desired volume and minimize disturbance with neighbouring contacts. A similar concept was successfully used to shorten arcing time by Cho et al [12].

A 1.5 mm thick steel plate was included in the simulation model as seen in Figure 3.6.

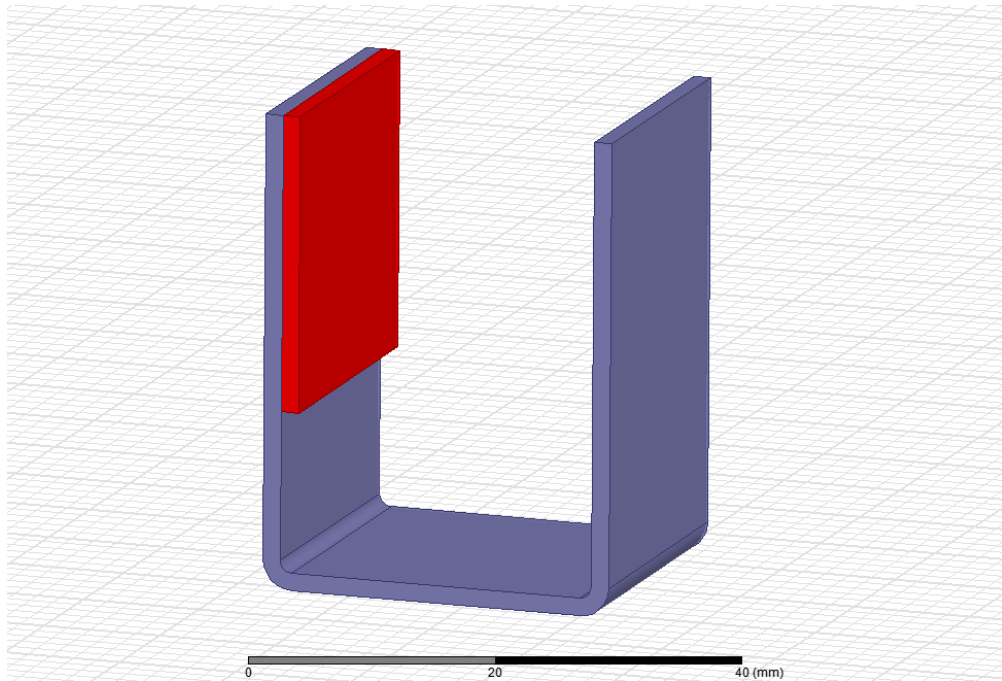
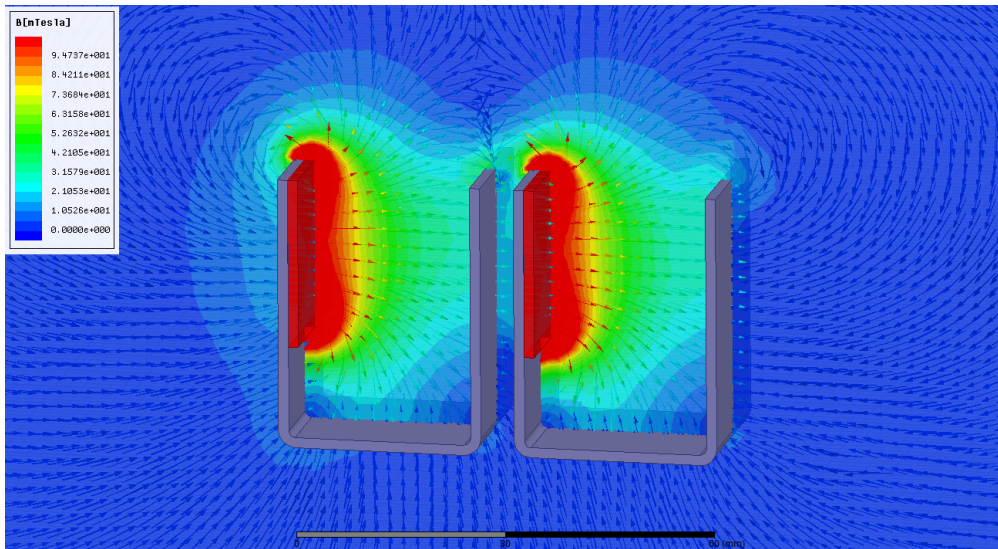
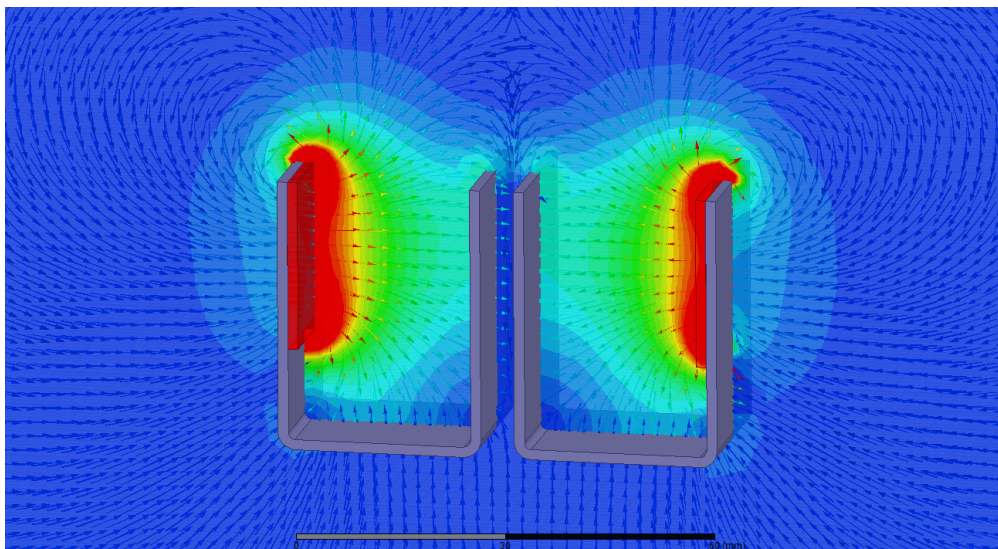


Figure 3.6: *Permanent magnet inside a U-shaped steel plate.*

Choosing a simple U-shape for the steel plates to use at each contact should simplify production. To verify that the concept work, a quick simulation was performed and the result shown in Figure 3.7. It appears from a visual view that most of the magnetic flux is concentrated within the enclosed volume of the metal plate. A comparison between Figure 3.7(a) and 3.7(b) shows a minimal disturbance between neighbours with different magnetic orientation. It is therefore of interest to study all configurations described in Section 3.3 both with and without metal plates for magnetic flux guidance.



(a) Magnet orientation: Right-Right



(b) Magnet orientation: Right-Left

Figure 3.7: Two magnets with metal plates located at the same distance as neighbouring poles in a size 5 contactor.

3.5 Simulation Models

In this section, simulation models for all configurations are explicitly shown. Eight magnets are used in each configuration and arranged in a manner to have the correct direction of magnetisation at each contact. All results are reported in Chapter 5.

3.5.1 Without Steel Plates

Similar to the simulation model of GAF185 in Section 3.2.2, neodymium magnets with the size $25 \times 25 \times 1.5$ mm are used. Magnet placement and orientations are chosen to suit each configuration.

RLRL

For the RLRL configuration, eight magnets were used and placed as shown in Figure 3.8.

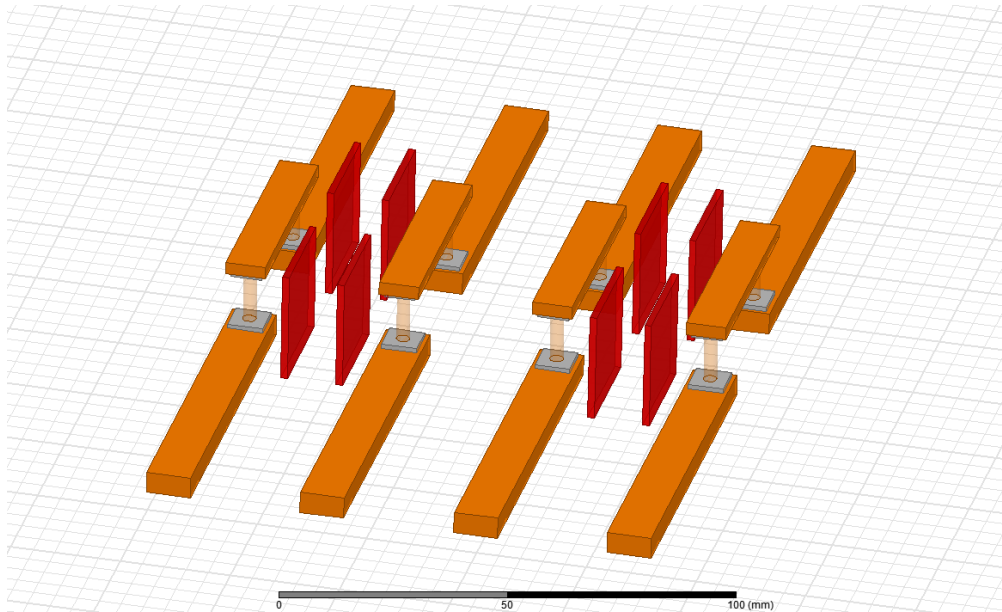


Figure 3.8: Configuration RLRL simulation model.

RLLR

For the RLLR configuration, eight magnets were used and placed as shown in Figure 3.9.

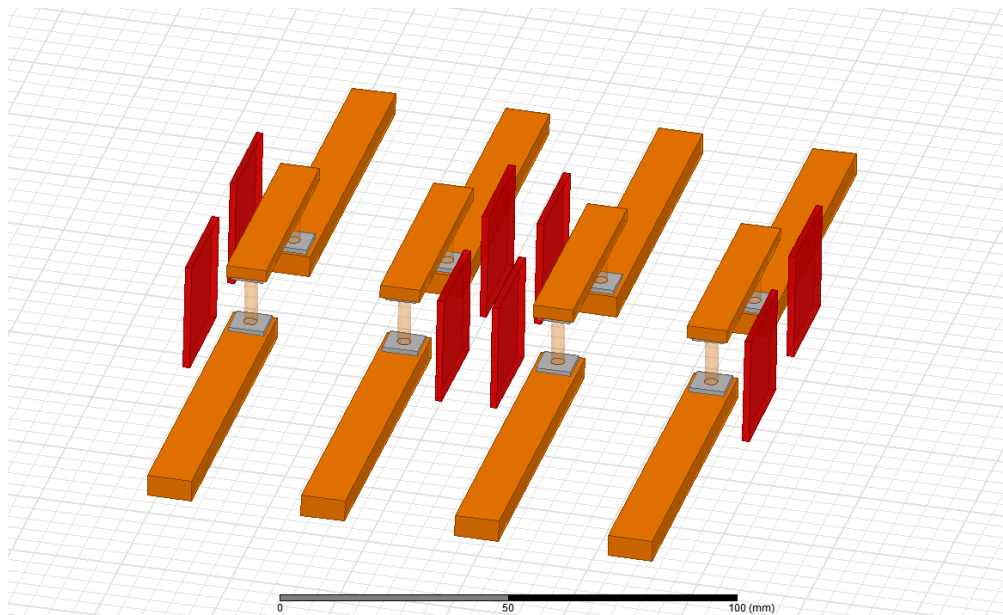


Figure 3.9: Configuration RLLR simulation model.

RRL

For the RRL configuration, eight magnets were used and placed as shown in Figure 3.9.

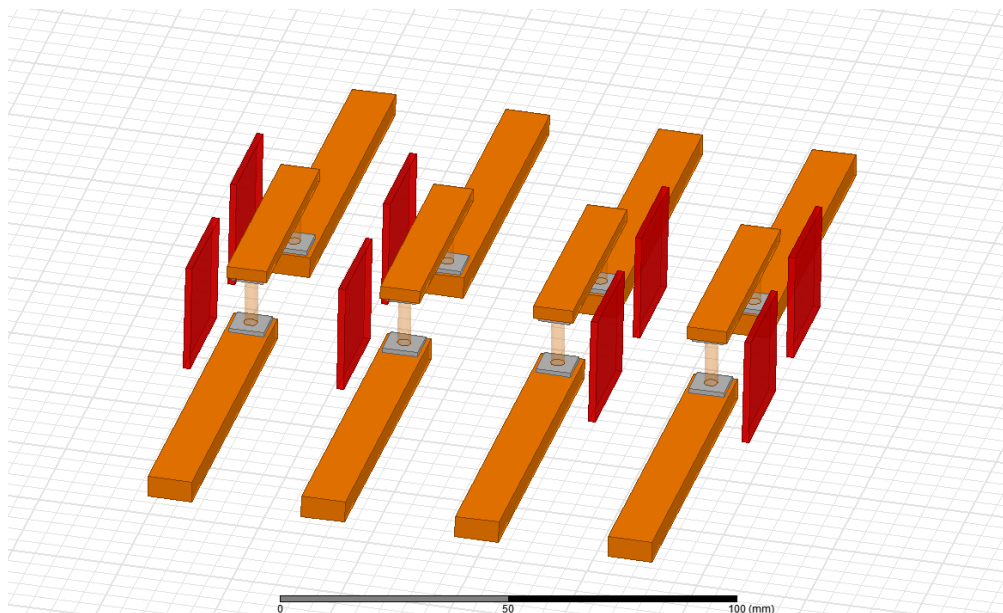


Figure 3.10: Configuration RLL simulation model.

3.5.2 With Steel Plates

In all configurations, one magnet and steel plate (shown in Figure 3.6) will be placed around each contact for a total of eight. The only difference for each configuration will be the orientation of the magnets.

RLRL

The simulation model for the RLRL configuration using steel plates is shown in Figure 3.11.

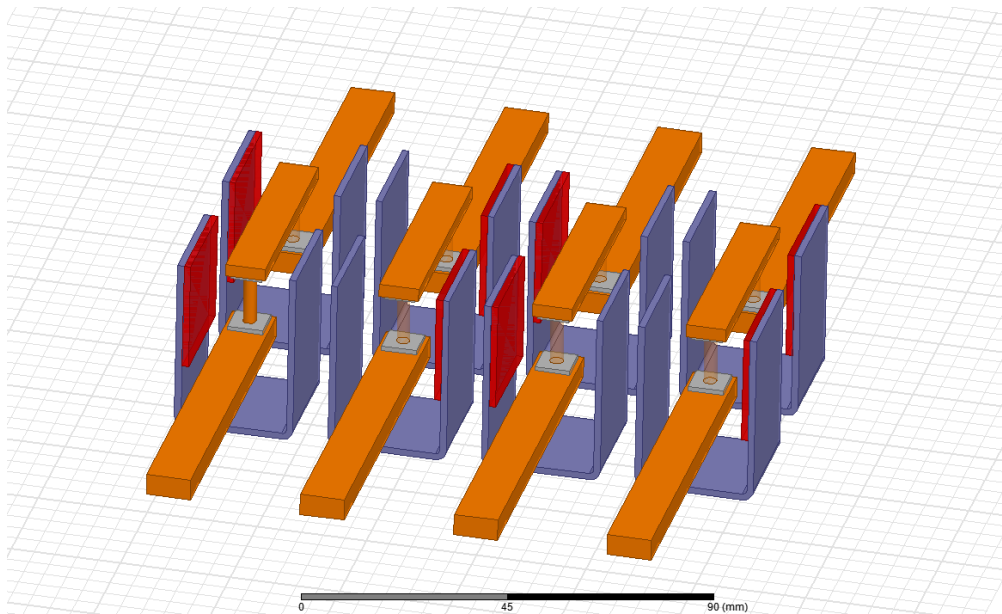


Figure 3.11: Configuration RLRL simulation model, with steel plates.

RLLR

The simulation model for the RLLR configuration using steel plates is shown in Figure 3.12.

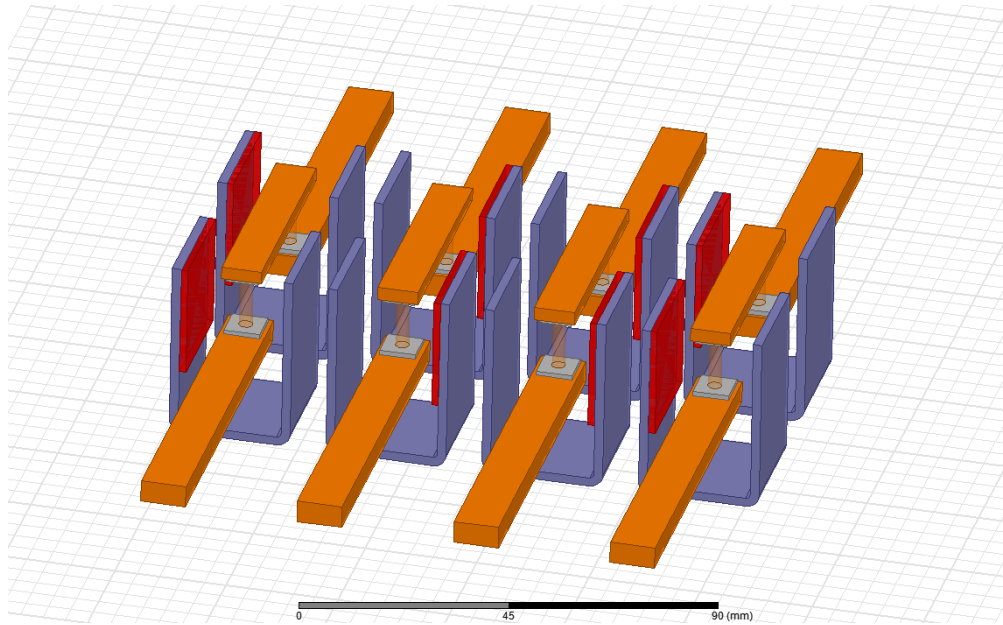


Figure 3.12: Configuration RLLR simulation model, with steel plates.

RRL

The simulation model for the RRL configuration using steel plates is shown in Figure 3.13.

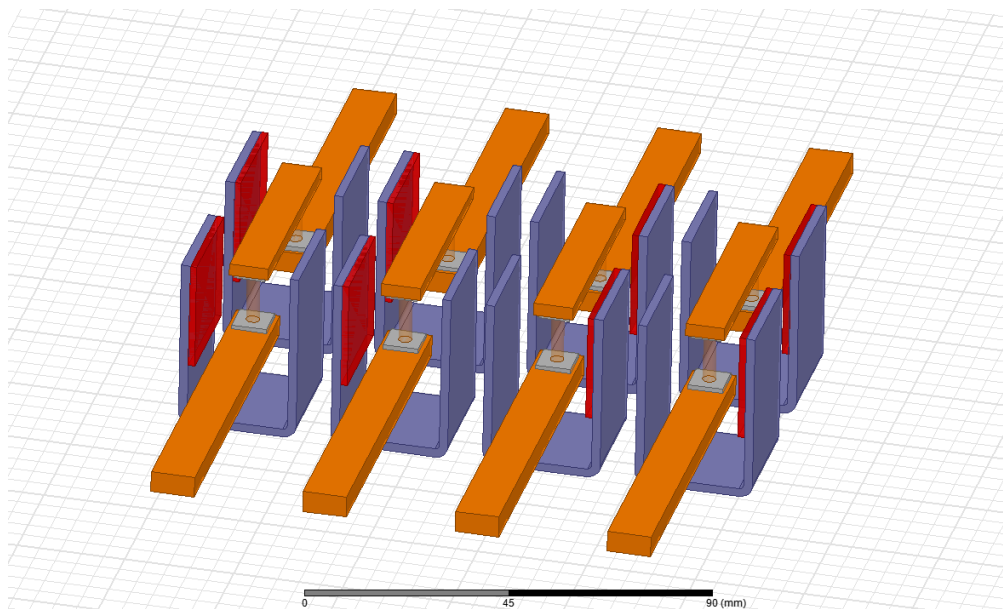


Figure 3.13: Configuration RRL simulation model, with steel plates.

4

ANSYS Simplorer Simulations

The second part of this thesis project is to implement a model of a DC contactor in ANSYS Simplorer. The model should simulate the current-voltage characteristics of the electric arcs.

4.1 About Simplorer

ANSYS Simplorer is an intuitive, multi-technology and multi-domain simulation program. It enables engineers to simulate electronically controlled systems and complex power electronic. It is capable of simulating all aspects of a large-scale system, from component level to system performance. Not only for electrical systems, but also mechanical and thermal systems. Simplorer is also able to perform co-simulations with other ANSYS programs making it an ideal tool for system modelling. The transient solver was used in this thesis to simulate the system behaviour over time.

4.2 DC Arc Model

The model of the contactor need not contain all aspects or parameters of the contactor, however it should have the proper current-voltage characteristics.

The idea is to use a resistor element to implement these characteristics. An electric arc does not behave like a resistor as the current-voltage dependence is non-linear and the slope of the curve is negative (see Equation (2.3)), although it has a conductance which depends on the length and current. By controlling the resistance with a function depending on current and time, the voltage across the resistor should resemble the arc voltage behaviour.

4.2.1 Free-burning Arc

For critical currents, the arc will not enter the arc chamber and the resistance will have the form as

$$R_{arc}(I_A, \Delta t) = \frac{U_A}{I_A} = \begin{cases} \frac{\Delta + (\tau + d) \cdot b \left(\ln \frac{I_A}{q} \right)^{-3}}{I_A} & \text{for } t > t_b \\ 0 & \text{for } t < t_b \end{cases} \quad (4.1)$$

where the contact distance (or arc length) d depends on time and the opening velocity ($d \approx v \Delta t$) and $\Delta t = t - t_b$ is the time lapsed after switching. The rest of the parameters were given in Section 2.1.5.

4.2.2 Arc inside Chamber

For higher currents, the arc will enter the arc chamber and the voltage increase will depend on the number of sub-arc. Since each sub-arc will contribute to about 25 V, the total voltage will be

$$U_{Chamber} = 25 \cdot N_{sub-arcs} \approx 25 \cdot \frac{v \Delta t}{d_{plates}} \quad (4.2)$$

For the proposed 4-pole size 5 contactor, the distance between the arc plates are 1.7 mm and the thickness is 1 mm which gives the total distance for each arc plate as $d_{plates} = 2.7$ mm. The characteristic resistance is of course given by $R_{Chamber} = \frac{U_{Chamber}}{I_A}$.

4.2.3 Arc Motion

The different voltage characteristics are determined whether or not the arc enters the arc chamber. The time it takes for the arc to reach the arc chamber depends on the current. Since no measurement data are available, it has to be modelled using a different method.

An arc formed in the center of the contact have to travel a distance of $s \approx 2$ cm to reach the arc chamber. The current-voltage characteristics of the arc will be

$$R_{arc} = \begin{cases} \frac{U_A}{I_A} & \text{for } s < 2 \text{ cm} \\ \frac{U_{Chamber}}{I_A} & \text{for } s \geq 2 \text{ cm} \end{cases} \quad (4.3)$$

The travelled distance is calculated by

$$s = \int v_{arc} dt \quad (4.4)$$

where the velocity, v_{arc} , varies for several different criteria as explained in Section 2.3.1. To summarize, v_{arc} is given by

$$v_{arc} = \begin{cases} 0 & \text{for } B \cdot d \cdot I_A^{0.63} < 9 \\ v_1 = 0.305 \cdot I_A^{0.6} B^{1.4} L^{2.22} & \text{for } B \cdot L^3 < 0.3 \\ v_2 = 0.176 \cdot I_A^{0.61} B^{0.74} & \text{for } B \cdot L^3 > 0.3 \\ v_3 = 1.80 \frac{J^{0.22} B^{0.5} I_A^{0.28}}{\rho^{0.5} L^{0.06}} & \text{for } B \cdot d \cdot I_A^{0.63} > 20 \end{cases} \quad (4.5)$$

The magnetic blast field described in Section 2.3 is dependent on the current flowing through the conductors. Due to the complex geometry it is not feasible to derive an analytical expression, but rather performing a numerical simulation. A model of a contact system with corresponding arc chamber (consisting of lamellae and arc runner made out of iron) was made in ANSYS Maxwell and shown in Figure 4.1.

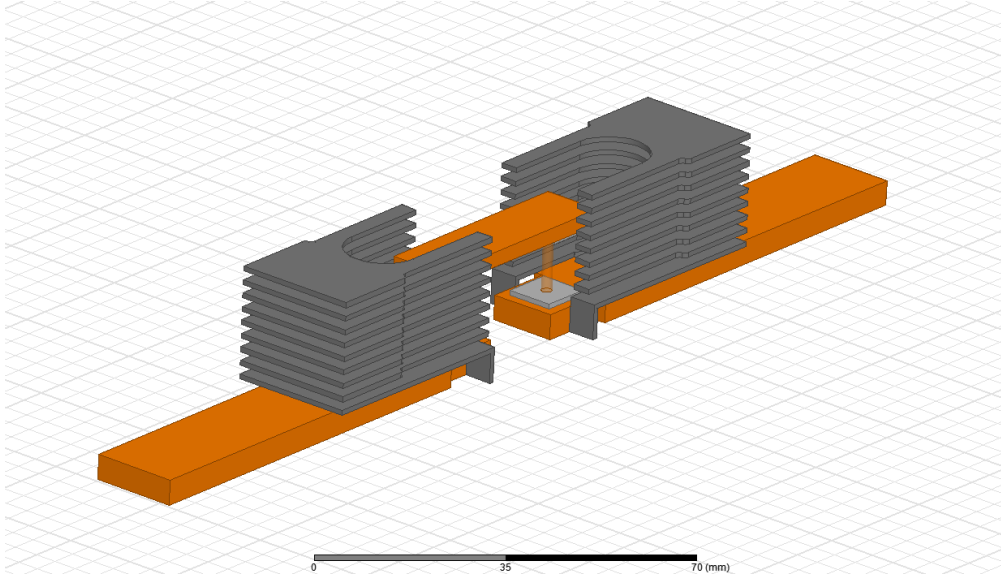


Figure 4.1: Maxwell simulation model for one contact system and arc chamber.

For each given current, the magnetic flux around the contact area was computed. The average B-field in the y-direction (which corresponds to the magnetisation direction in Figure 2.4) was calculated for currents up to 100 A and opening distances up to 1.2 cm and plotted in Figure 4.2. For each opening distance the result shows a linear dependence of current

$$B = f(d) \cdot I_A \quad (4.6)$$

Where $f(d)$ turns out to contain a weak opening distance dependence with $f(d) = 0.029642 - 0.00094d$. In summary, the magnetic blowout field, B [mT], can be expressed in terms of opening distance, d [cm], and current, I_A [A]:

$$B = (0.029642 - 0.00094d) \cdot I_A \quad (4.7)$$

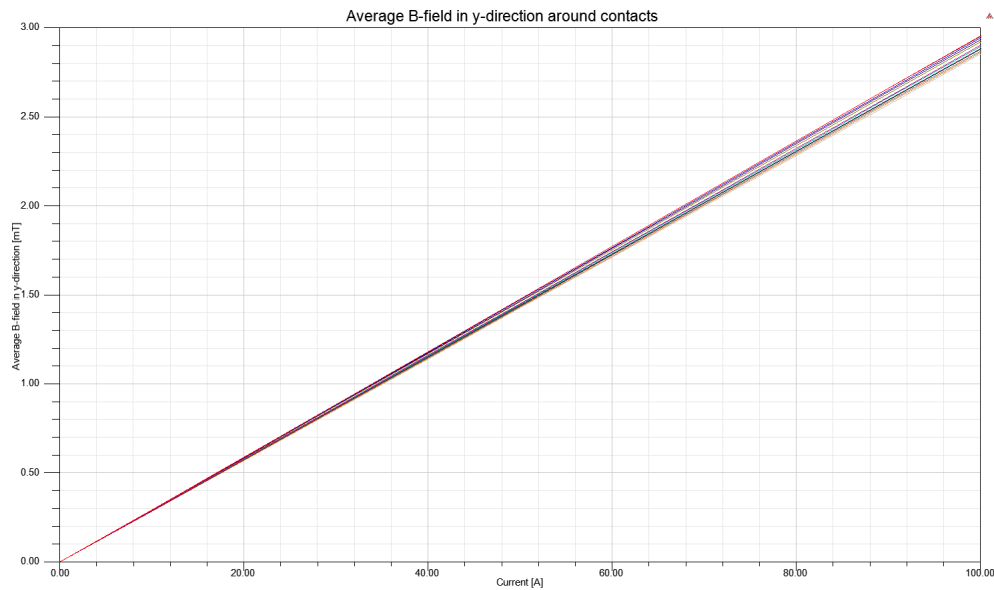


Figure 4.2: Calculated magnetic blowout field as a function of current.

4.3 Simplorer Model

A simple model of one contact inside the contactor is shown in Figure 4.3. The elements in the model are described below

1. **The control logic** will, after a certain predetermined *breaktime*, switch the contactor *off*.
 - (a) Breaking process starts and the arc will be free-burning between the contacts.
 - (b) The magnetic field is sufficiently strong to allow arc mobility according to criteria (2.14). The arc velocity is to be v_1 according to Equation (4.5).
 - (c) Arc velocity is no longer gap dependent and set to be equal to v_2 .
 - (d) Criteria (2.13) is met and the arc will have continuous motion. Arc velocity is set to v_3 .
 - (e) The arc has reached the arc chamber. Current-voltage characteristics are adjusted according to (4.3).
2. **The Equation Block** contains all the parameters and functions that controls the current-voltage characteristics of the arc.
3. An **amp-meter** measures the arc current, which is used in the equation block to control the characteristic resistance across the contacts.

4. As the current drop to zero, the characteristic resistance will approach $\pm\infty$. The **Controlled switch** is used to interrupt the circuit when current drops below a minimum value to ensure stability in the simulations.
5. The **Controlled Resistor Element** is the main component in the model and it is used to imitate the current-voltage characteristics of the separating contacts. One pole consists of two contacts therefore the total resistance is set to be $R = 2 \cdot R_{arc}$.
6. A **voltmeter** measures the voltage across the contact. Not used in the simulations but for analysing the results.
7. **DC voltage source**.
8. Since $R_{arc} = 0$ before switching the contacts are assumed to be perfect conductors. The rated current in the circuit is determined by the supply voltage, U_0 , and the **Load Resistor Element** R_{Load} as simply $I_0 = \frac{U_0}{R_{Load}}$.

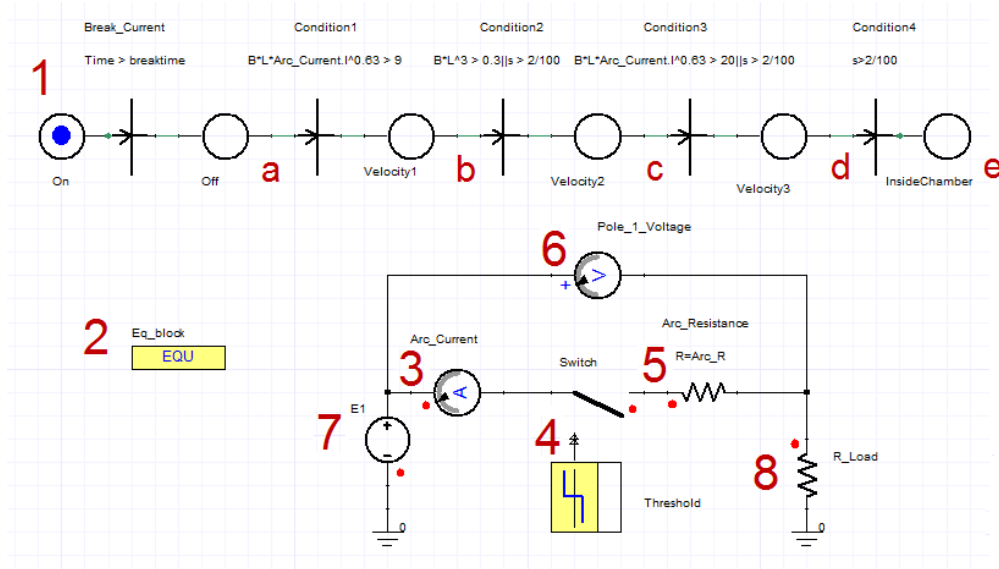
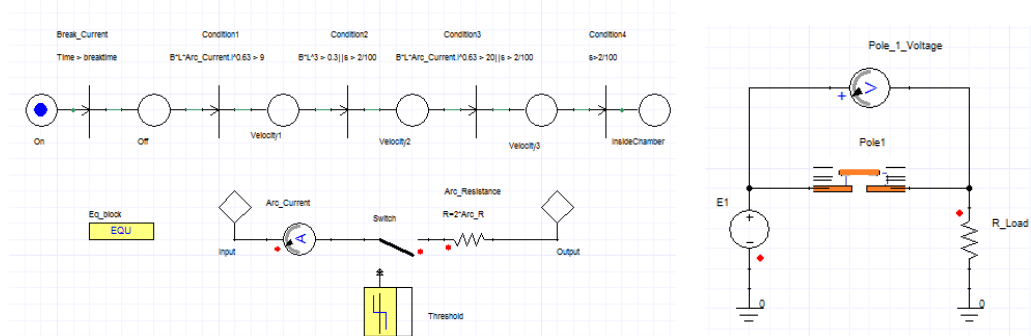


Figure 4.3: ANSYS Simplerer workbench for a 1-pole DC arc model.

1-5 consists consists of the elements and controls to model the contact. These could be exported to sub-circuit to clean up the workbench. The sub-circuit is shown in Figure 4.4(a) and new overview of the model is shown in Figure 4.4(b).



(a) Elements exported to a sub-circuit.

(b) Simple circuit with the pole component.

Figure 4.4: ANSYS Simplorer workbench with the use of sub-circuits.

4.4 4-Pole Model

The 1-pole component from the previous section is used to extend to model to account for a contactor with four poles and is shown in Figure 4.5. The new elements in the model are described below

1. Each component represents one **pole** modelled in the previous chapter.
2. A **voltmeter** measures the voltage across the contactor.
3. **DC voltage source** set to 1500 V.

The poles in Figure 4.5 are connected in series for the purpose of this thesis.

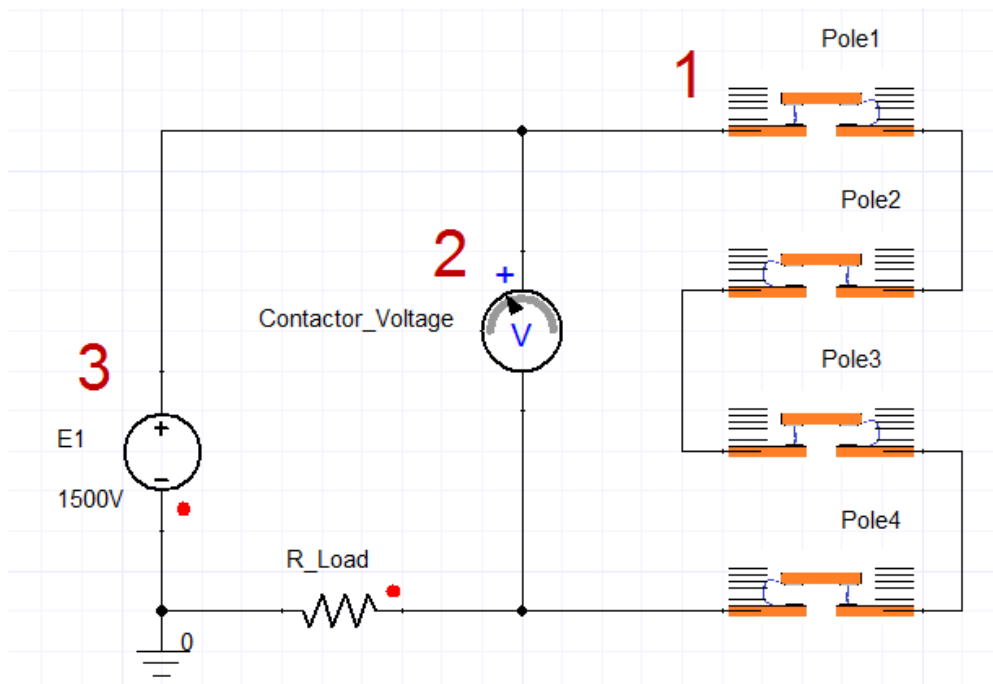


Figure 4.5: ANSYS SImplorer workbench for a 4-pole contactor with DC arc model.

5

Maxwell Simulation Results

Results from the simulation models described in Chapter 3 are presented in this chapter. Magnetic field plots are shown for each configuration in Section 3.5 and a numerical summary is presented in Section 5.4.

5.1 GAF185

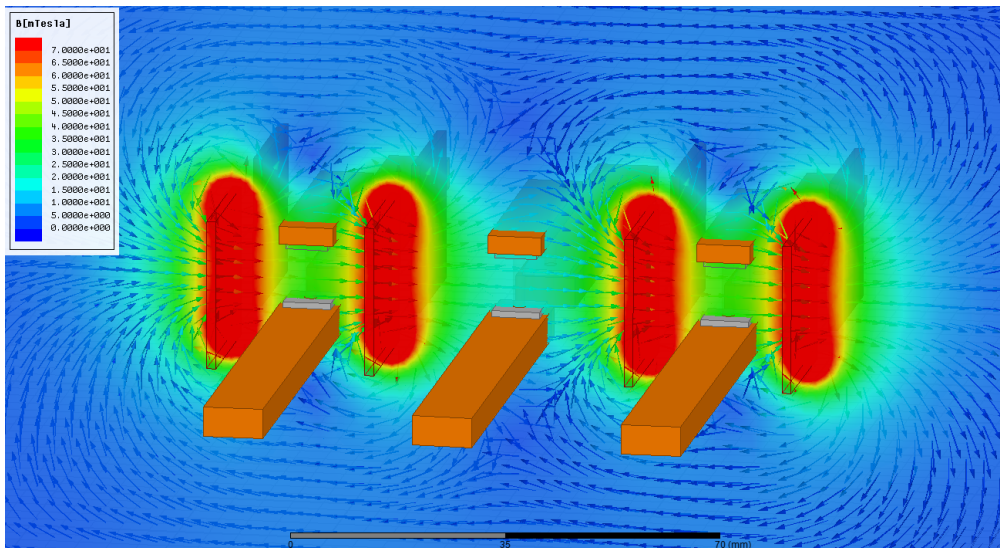


Figure 5.1: *GAF185 simulation results visualizing B-field direction and magnitude.*

5.2 w/o Steel Plates

Results from simulation models in Section 3.5.1 are presented below. A summary is given in Section 5.4.

5.2.1 RLRL

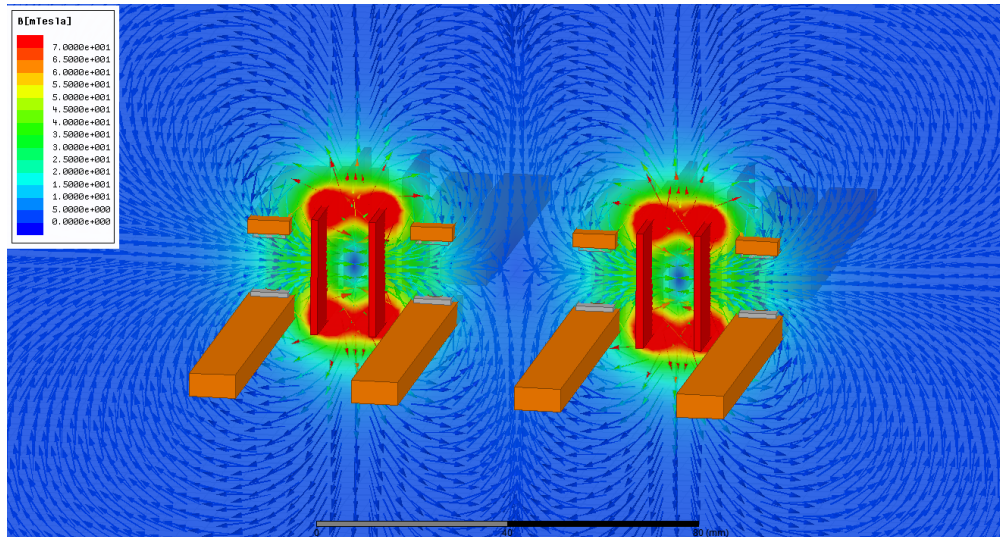


Figure 5.2: Configuration RLRL simulation results visualizing B -field direction and magnitude.

5.2.2 RLLR

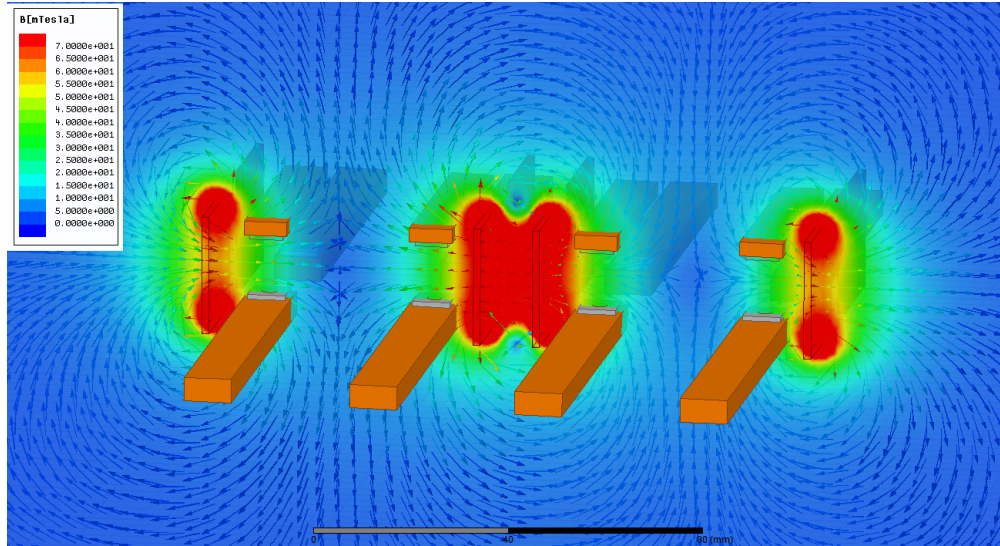


Figure 5.3: Configuration RLLR simulation results visualizing B-field direction and magnitude.

5.2.3 RRLR

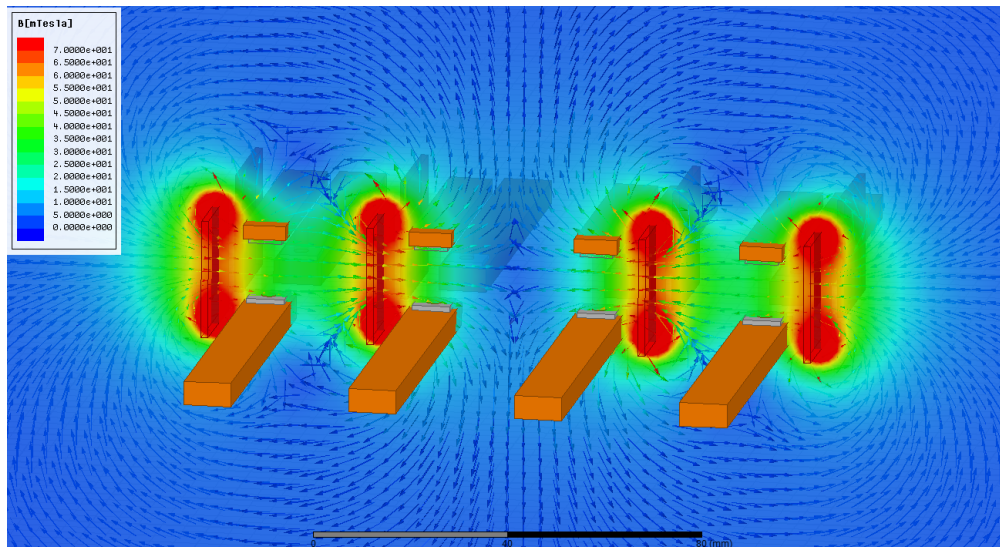


Figure 5.4: Configuration RRLR simulation results visualizing B-field direction and magnitude.

5.3 With Steel Plates

Results from simulation models in Section 3.5.2 are presented below. A summary is given in Section 5.4.

5.3.1 RLRL

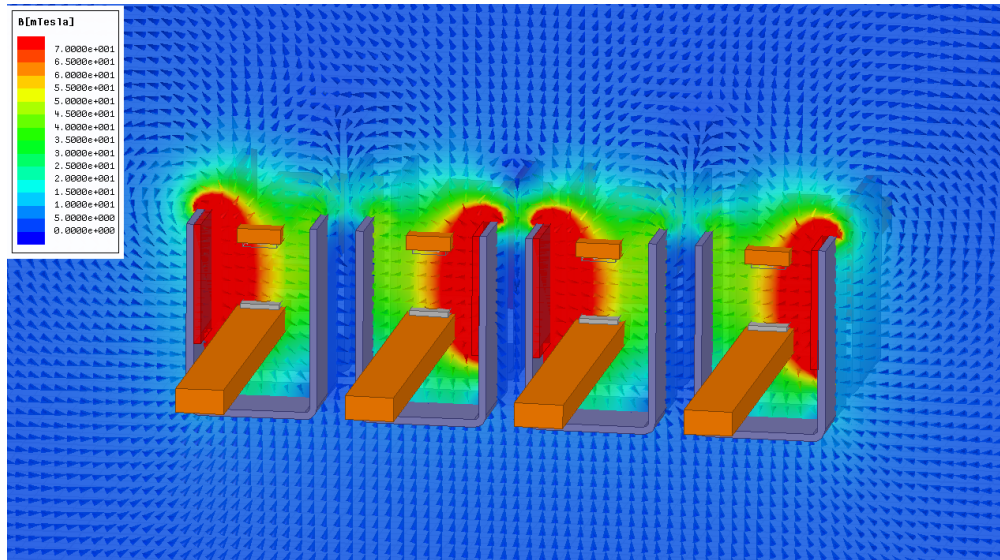


Figure 5.5: Configuration RLRL with steel plates simulation results visualizing B-field direction and magnitude.

5.3.2 RLLR

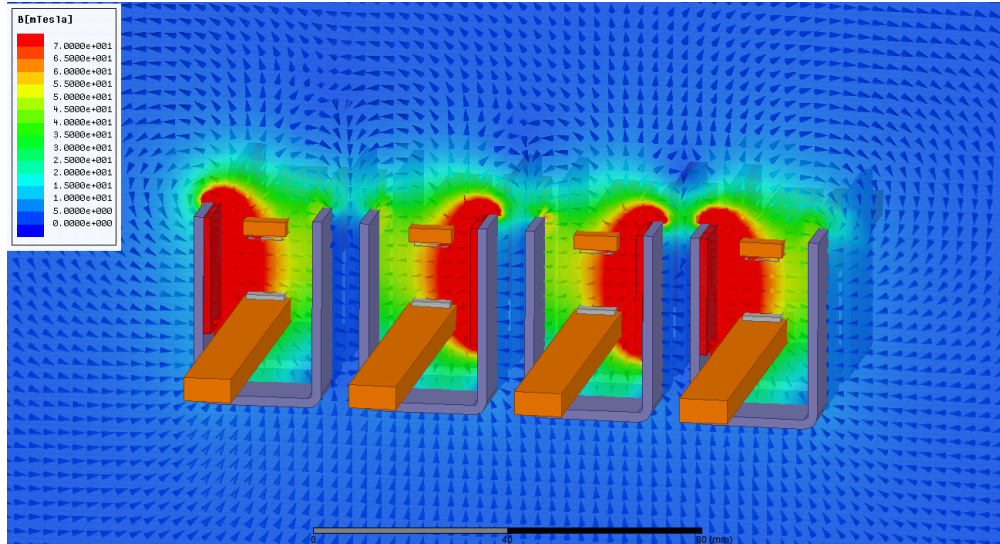


Figure 5.6: Configuration RLLR with steel plates simulation results visualizing B-field direction and magnitude.

5.3.3 RRLI

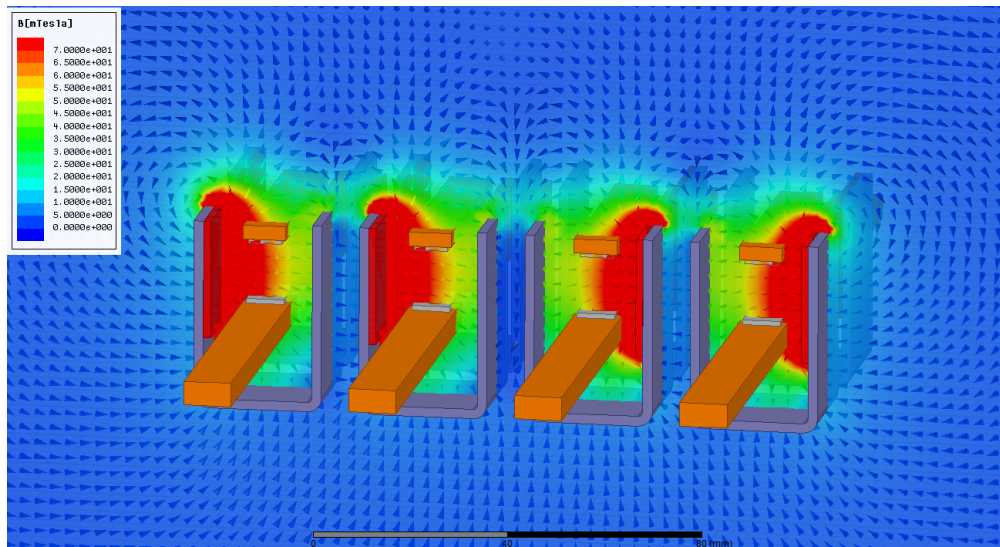


Figure 5.7: Configuration RRLI with steel plates simulation results visualizing B-field direction and magnitude.

5.4 Summary

The average magnetic flux at each contact is calculated using Equation (3.2). Due to symmetry, the two contacts at the same pole will have the equal magnetic flux. Therefore only one value for each pole is presented in Table 5.1. The numerical sign of the values in table 5.1 are relative the desired magnetic direction, not the y-direction when calculating $\langle B_y \rangle$.

To compare the different configurations, it is useful to calculate the average magnetic flux per pole

$$\overline{B_y} = \frac{\sum_{poles} \langle B_y \rangle}{N_{poles}} \quad (5.1)$$

Poles with a negative value have the wrong direction of magnetization and will not contribute to the breaking process and is therefore not included when calculating $\sum_{poles} \langle B_y \rangle$. The efficiency of the design also depends on how many magnets are used per pole (3.1). A relevant comparison is therefore

$$\frac{\overline{B_y}}{V_{Magnets}/N_{Poles}} = \frac{\sum_{poles} \langle B_y \rangle / N_{poles}}{V_{Magnets}/N_{Poles}} = \frac{\sum_{poles} \langle B_y \rangle}{V_{Magnets}} \quad (5.2)$$

The ratio gives the effective magnetic flux per cubic centimeter of magnetic material used. All configurations uses eight magnets of the same size, therefore $V_{Magnets} = 8 \cdot 2.5 \text{ cm} \times 2.5 \text{ cm} \times 0.15 \text{ cm} = 7.5 \text{ cm}^3$.

Metal Plates	Config.	$\langle B_y \rangle$ [mT]				Index
		Pole 1	Pole 2	Pole 3	Pole 4	
Without	GAF185	45.8	-15.0	45.8	-	100
Without	RLRL	19.6	18.8	18.8	19.6	83.6
Without	RLLR	24.6	32.5	32.5	24.6	124.6
Without	RRLR	34.0	26.6	26.6	34.0	132.8
With	RLRL	60.6	60.6	60.6	60.6	264.8
With	RLLR	64.6	64.6	64.6	64.6	282.8
With	RRLR	64.5	64.6	64.6	64.5	282.0

Table 5.1: Summary and comparison of results from Chapter 5.

6

Simplorer Simulation Results

Results from the simulation models described in Chapter 4 are presented in this chapter. Circuit currents are swept between 0 – 150 A. The system is allowed 100 ms to stabilize before the contactor switches *off* and breaking process begins. The simulations run for an additional 100 ms to determine which currents are critical.

6.1 1-Pole Model

The 1-pole model is described in Section 4.3. The voltage and current after the time of breaking is shown in Figure 6.1 and 6.2 for several different circuit currents.

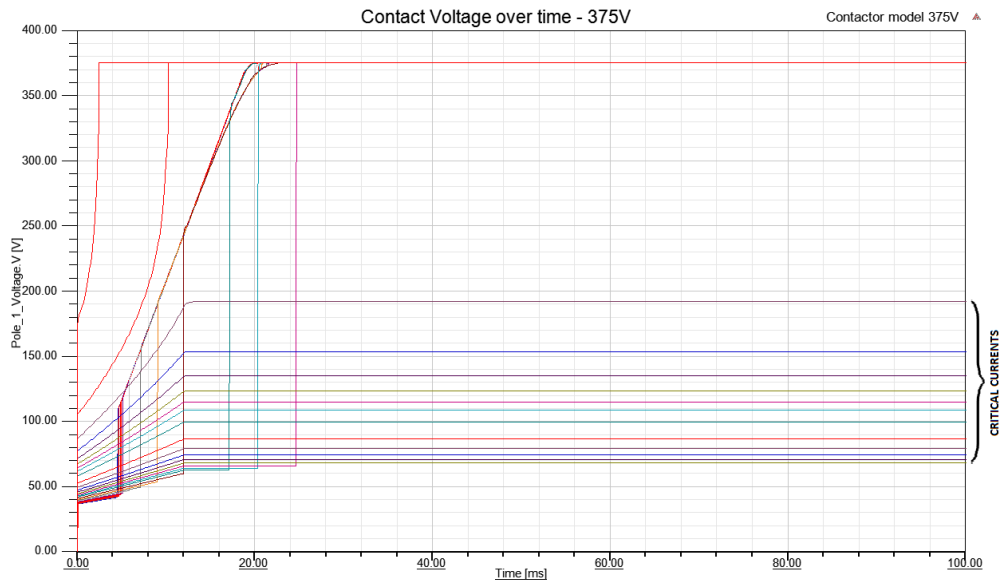


Figure 6.1: Voltage across one contact system over time.

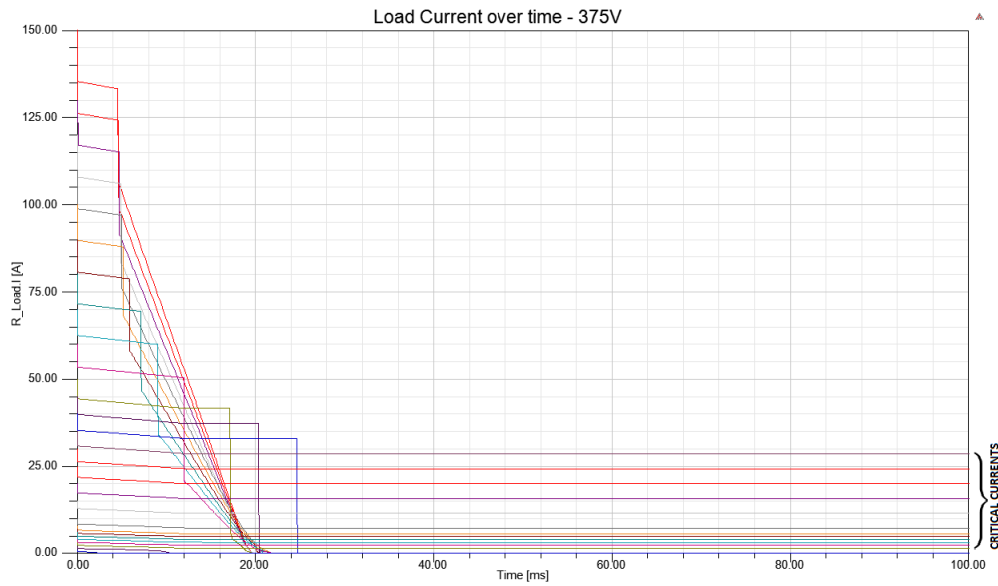


Figure 6.2: Load current over time.

Quick jumps in voltage and current represents an arc entering the arc chamber. Curves not reaching 0 A or 375 V (marked in the figures) represents arcs not completely extinguished. Figure 6.3 shows breaktimes as a function of circuit current.

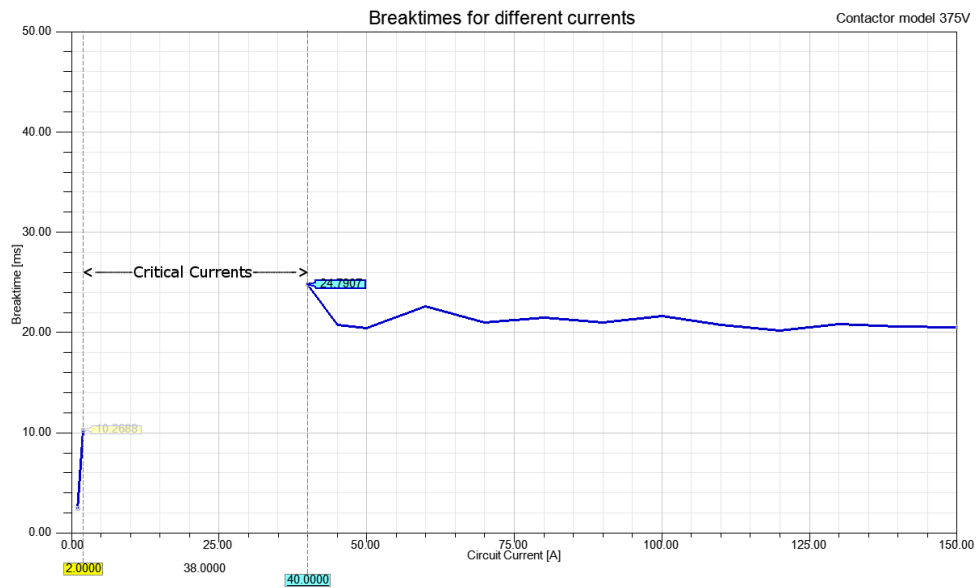


Figure 6.3: Breaktimes for circuit currents between 0 – 150 A.

6.2 4-Pole Model

The 1-pole model is extended to a 4-pole model as described in Section 4.4. The voltage and current after the time of breaking is shown in Figure 6.4 and 6.5 for several different circuit currents.

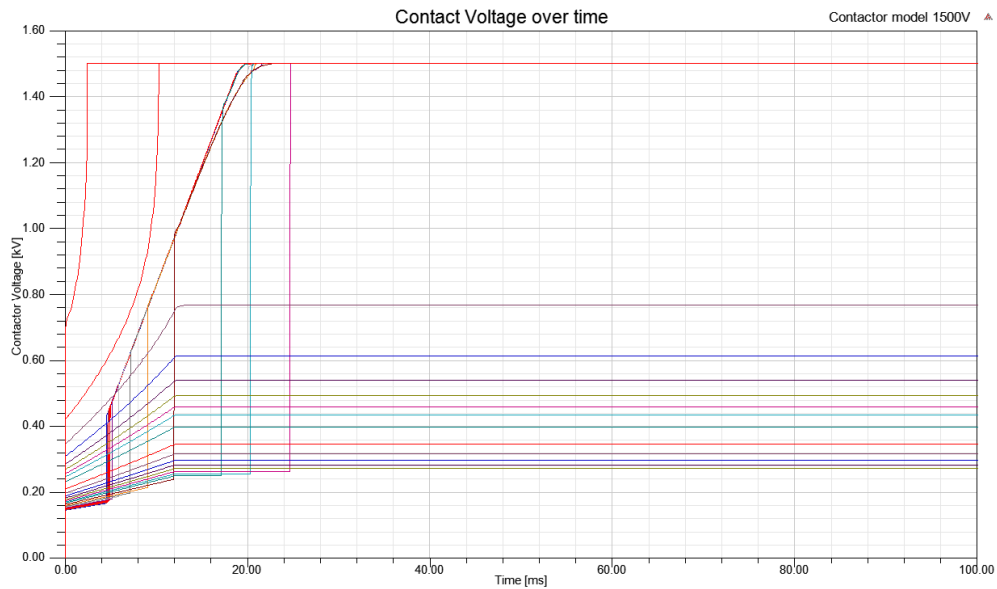


Figure 6.4: Voltage across all four poles over time.

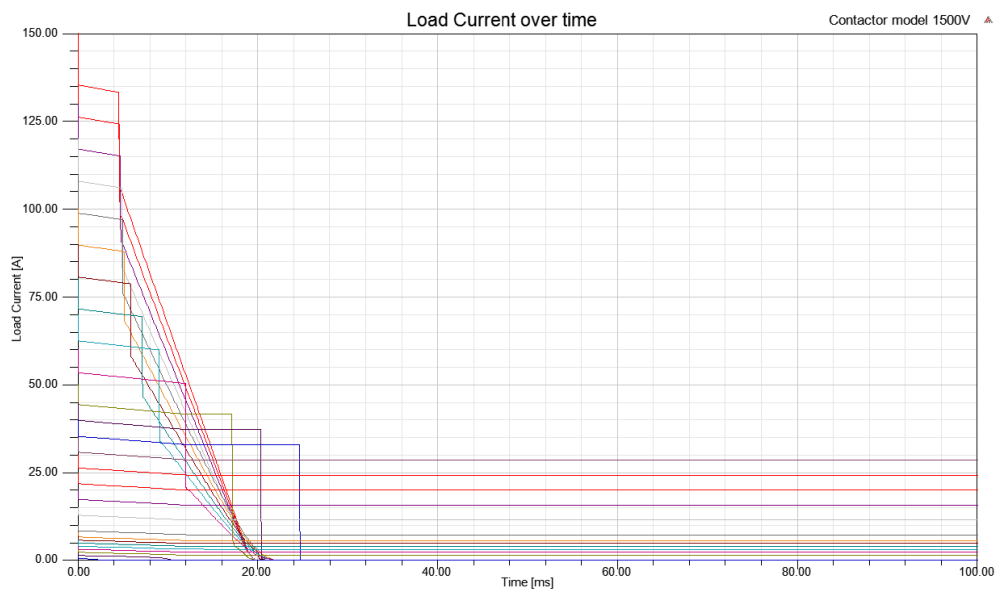


Figure 6.5: Load current over time.

The results are similar to the 1-pole model as expected, however the total voltage across all poles are set to 1500 V, corresponding to 375 V per pole. Breaktimes are shown in Figure 6.6.

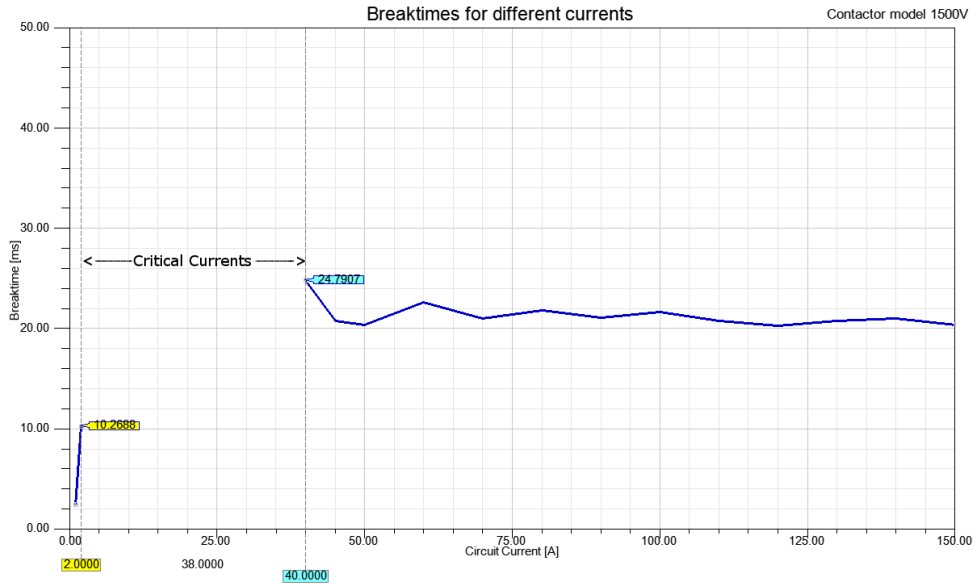


Figure 6.6: Breaktimes for circuit currents between 0 – 150 A.

7

Discussion

The results from Chapter 5 and 6 gives rise to some interesting points of discussion and will be discussed separately.

7.1 Part I

The different proposed placement and arrangement of magnets all show promising result compared to the already existing GAF185, with only the RLRL configuration being less efficient. This is because the alternating directions of magnets is very difficult to achieve without using too many magnets. However, RLLR and RRLR show an increase in efficiency with 24.6% and 32.8%, where as the configurations with steel plates show an increase with 164.8 – 182.8 %.

The comparison index only considers the total magnetic flux at all poles and does not consider the variation across the different poles. In reality, having a very strong magnetic field at one pole is irrelevant for another pole if $\langle B_y \rangle$ does not exceed a minimum value. To ensure that enough magnetic flux is available at each pole it is useful to estimate a minimum value. The Simpler simulations result of a 1500V contactor, presented in Section 6.2, shows that currents lower than 2 A are not self-sustainable. Using criteria (2.13) it is possible to calculate a lower limit for the magnetic flux which would allow reliable magnetic blowout for all currents above 2 A:

$$B_{min} = \frac{20}{d_{max} \cdot I_{cc,min}^{0.63}} \approx \frac{20}{1.2 \cdot 2^{0.63}} \approx 11 \text{ mT} \quad (7.1)$$

To be on the safe side it would be wise to design for a higher minimum value around $2 \cdot B_{min} \approx 20 \text{ mT}$.

The steel plates configurations all have more 60 mT at each pole which is more than three times the minimum value, allowing plenty of room for design. The magnet sizes could be significantly reduced and still be sufficient. Although the RLLR and RRLR

configurations with steel plates have the highest comparison indices, the RLRL allows for the simplest wiring to connect all the poles in series. Without steel plates, the RLLR and RRLR are the most promising.

7.1.1 Conclusions

It is possible to use permanent magnets in a 4-pole DC contactor to efficiently extinguish the electric arcs. To do this, the magnetic flux from the permanent magnets has to generate at least 11 mT in the right direction at each contact and a minimum of 7 lamellae are required in each arc chute.

The best solution uses steel plates surrounding the magnet and contact system to increase the magnetic flux density and reduce destructive interference between magnets of neighbouring poles. This reduces the volume of magnets required and the magnet orientation can be chosen arbitrarily at each pole, making it possible to construct the contactor to be wired in the simplest way.

Without using steel plates, the most efficient configuration is RLLR corresponding to a wiring shown in Figure 3.5(b). The alternating fields at the two poles on either side, RL and LR, allows for simple connection to use the contactor as a 2×2 pole contactor at 750 V.

7.1.2 Recommendations for future work

Since this thesis work is a pre-study of suitable technical solutions, plenty of work lies ahead. Parallel to this thesis work another student, *Markus Angell* at Mälardalens Högskola, has been working on his thesis project to implement the solutions into the construction of the contactor. The next step would be to use the results from these two theses to construct a prototype to verify the simulation results. Most interesting to verify is the new concept using steel plates for magnetic flux guidance.

7.2 Part II

The implemented DC arc model is able simulate the current-voltage characteristics that agree quite well to the measurement data currently available at ABB. All this even though most of the equations and criteria used were found in publications from the 1950s and 1960s. Most interesting aspect of the model is that it predict critical currents.

A few substantial simplifications has been made in the model which needs to be discussed.

- The arc is assumed to be a straight cylindrical conductor and the arc length is assumed to the same as the opening gap distance. Any bending of the arc is not taken into account.
- All geometry dependencies are excluded. Geometry around the contacts plays a huge role in where the arc is formed and how it mobilizes. In the model, the arc is assumed to have a straight path to reach the arc chamber 2 cm away.
- The arc is assumed to split into sub-arcs between the lamellae as soon as it reaches the arc chamber. In reality, the arcs ability to enter the arc chamber is a complicated process to model which also depends on the velocity it enters the arc chamber with.

Taking these remarks into account, it is plausible that the span of critical current is broader in reality than the simulation results indicate.

7.2.1 Conclusions

The DC arc model is successful and predicts a span of critical current. Any number of poles could be added and wired arbitrarily to simulation the switching capabilities of the contactor. The contactor model could be connected to any circuit or system.

7.2.2 Recommendations for future work

Add inductive loads to the model in accordance to the utilization category and evaluate the switching performance.

Once a prototype has been built, compare the measurement data to the simulation results to evaluate the model.

Recommendations for future use of the model will not be discussed in this thesis in accordance with the non-disclosure agreement.

Bibliography

- [1] S. Lee, Hyosung-Kim, *A study on Low-Voltage DC circuit breakers*, in: 2013 IEEE International Symposium on Industrial Electronics, Institute of Electrical and Electronics Engineers, 2013, pp. 1–6.
- [2] ABB Automation Technologies AB, Cewe-Control, *A/AF kontaktorer - Det perfekta valet*, 1SFC101001B3401 (March 2004).
- [3] P. G. Slade, *Electrical Contacts: Principles and Applications (Electrical Engineering and Electronics)*, CRC Press, 1999.
- [4] T. Mori et al, *A New Interruption Method for Low-Voltage, Small-Capacity, Air-Break Contactors*, IEICE Transactions on Industry Applications 27 (1) (1991) 161–166.
- [5] A. Eidinger, W. Rieder, *Das Verhalten des Lichtbogens im transversalen Magnetfeld*, Archiv für Elektrotechnik 43 (1957) 94–114.
- [6] E. Philippow, *Taschenbuch Elektrotechnik*, VEB Verlag Technik Berlin, 1965-1969, pp. 397–400.
- [7] H. Kim, *Arcing characteristics on low-voltage DC circuit breakers*, Institute of Electrical and Electronics Engineers, 2013, pp. 1–7.
- [8] K. Yoshida, K. Sawa, K. Suzuki, M. Watanabe, H. Daijima, *Influence of Voltage and Current on Arc Duration and Energy of DC Electromagnetic Contactor*, Institute of Electrical and Electronics Engineers, 2011, pp. 1–5.
- [9] T. Atsumi, J. Sekikawa, T. Kubono, *Characteristics of Break Arcs Driven by Transverse Magnetic Field in a DC High-Voltage Resistive Circuit*, IEICE Transactions on Electronics E93-C (9) (2010) 1393–1398.
- [10] D. Alferov, G. Belkin, D. Yevsin, *DC vacuum arc extinction in a transverse axisymmetric magnetic field*, in: 2008 23rd International Symposium on Discharges and Electrical Insulation in Vacuum, Institute of Electrical and Electronics Engineers, 2008, pp. 402–405.

- [11] J. Sekikawa, T. Kubono, *Characteristics of Break Arcs Driven by External Magnetic Field in a DC42V Resistive Circuit*, in: 2008 Proceedings of the 54th IEEE Holm Conference on Electrical Contacts, Institute of Electrical and Electronics Engineers, 2008, pp. 21–26.
- [12] H. Cho, E. Lee, *DC Arc extinction using external magnetic field in switching device*, in: The 30th International Conference on Plasma Science, 2003. ICOPS 2003. IEEE Conference Record - Abstracts., Institute of Electrical and Electronics Engineers, 2003, p. 139.